# STUDY ON SHAPE SEPARATION OF PARTICULATE MATERIALS

大矢, 仁史

https://doi.org/10.11501/3132443

出版情報：九州大学, 1997, 博士（工学）, 論文博士
バージョン：
権利関係：

# Chapter 4. INCLINED CONVEYOR

## 4.1 Introduction

This chapter deals with the third particle shape separator, which was developed as a new type of separator. It is called an inclined conveyor.

It consists of a moving flat plate like a belt conveyor, which is included in the rolling or sliding type. An inclination angle is necessary to give different trajectories to the spherical particles compared with the nonspherical particles.

The movement of the plate for a prototype of this method is the same direction to its inclination[18] as if it were an inclined rotating disk method[20-22] and a rotating cone method[25-27]. However, nonspherical particles retained on the plate easily protect the movement of the spherical particles. This is similar to an inclined rotating disk and an inclined vibration plate. The direction of inclination was improved to be perpendicular to the movement of the plate as shown in Fig. 4.1.

Particles close to spherical shape can be considered to have a smaller coefficient of friction and rapidly roll down to the lower side as trajectory 1. Nonspherical particles which have a larger coefficient of friction tend to stay on the belt and are transported by a conveyor as trajectory 2. The separation by this apparatus is performed using the difference in the trajectories of the spherical and nonspherical particles on the belt.

Motions of spherical and nonspherical particles will be discussed at various levels of the belt speed and the inclination angle.

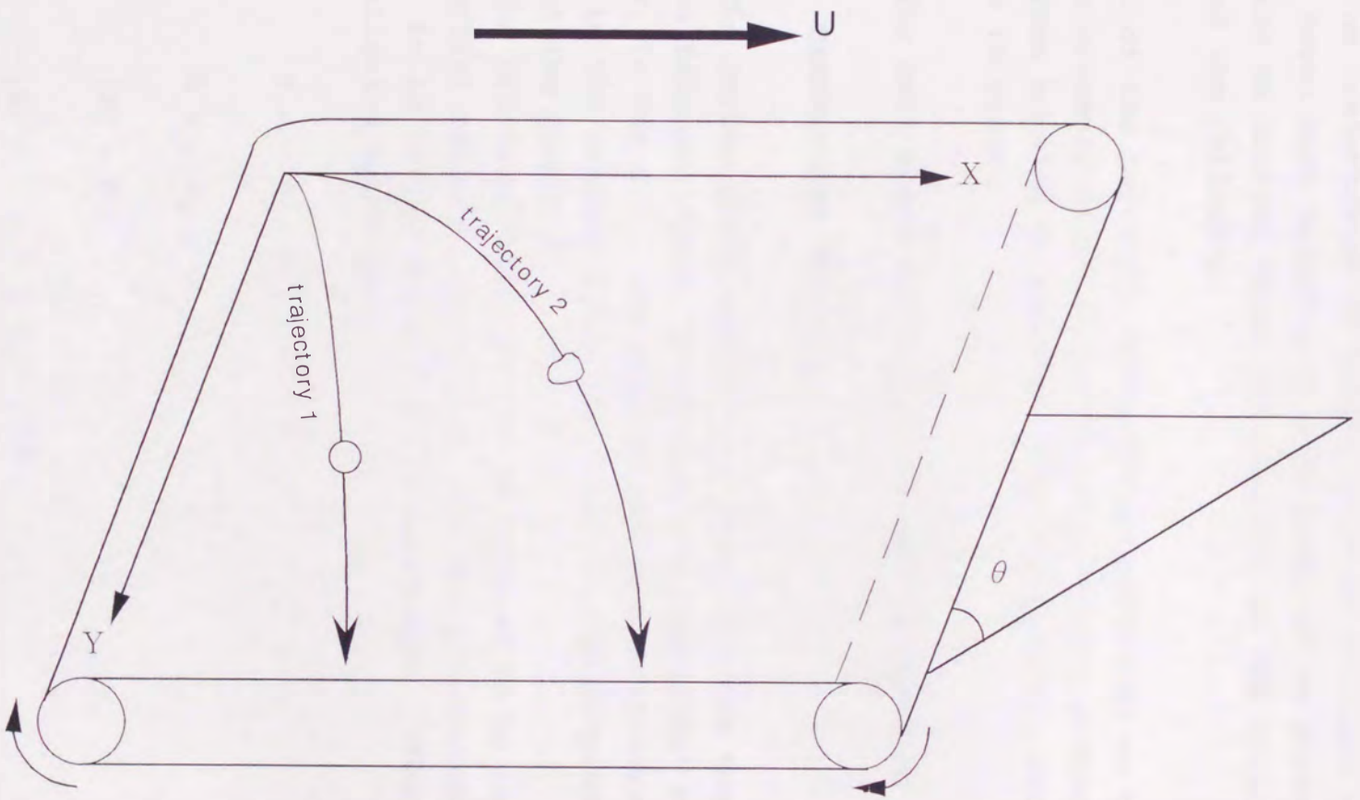


Fig. 4.1 Inclined conveyor

## 4.2 Theory on trajectory of particles

### 4.2.1 THEORETICAL MODEL

The trajectories of particles on an inclined flat plate, which moves with velocity U, were examined as shown in Fig.4.1. We tried to analyze these trajectories on the moving belt and assumed the following:

1. All of the particles are material particles on the movement.
2. The movement of particles is only sliding without bounding.
3. Forces working on the particles are gravity, resistance and friction.

The belt speed was U m/s, and the inclination angle was $\theta$.

### 4.2.2 THEORETICAL ANALYSIS

The forces which work on the particles are the gravity, mg, and the friction force, **R**, against the particles' relative velocity, **v**, in Fig.4.2. The gravity was separated into a partial force in the sloping direction and in the perpendicular direction of the plate, **N**.

The friction force, **R**, can be assumed to be in proportion to the partial force of gravity, **N**, and the proportional coefficient is $\mu$. It is called the friction coefficient. These are given in the following equations:

$$\mathbf{F} = ( 0 , F ) \tag{4-1}$$

$$\mathbf{R} = ( R_x , R_y ) \tag{4-2}$$

$$|\mathbf{F}| = F \tag{4-3}$$

$$|\mathbf{R}| = ( R_x^2 + R_y^2 )^{1/2} = \mu |\mathbf{N}| \tag{4-4}$$

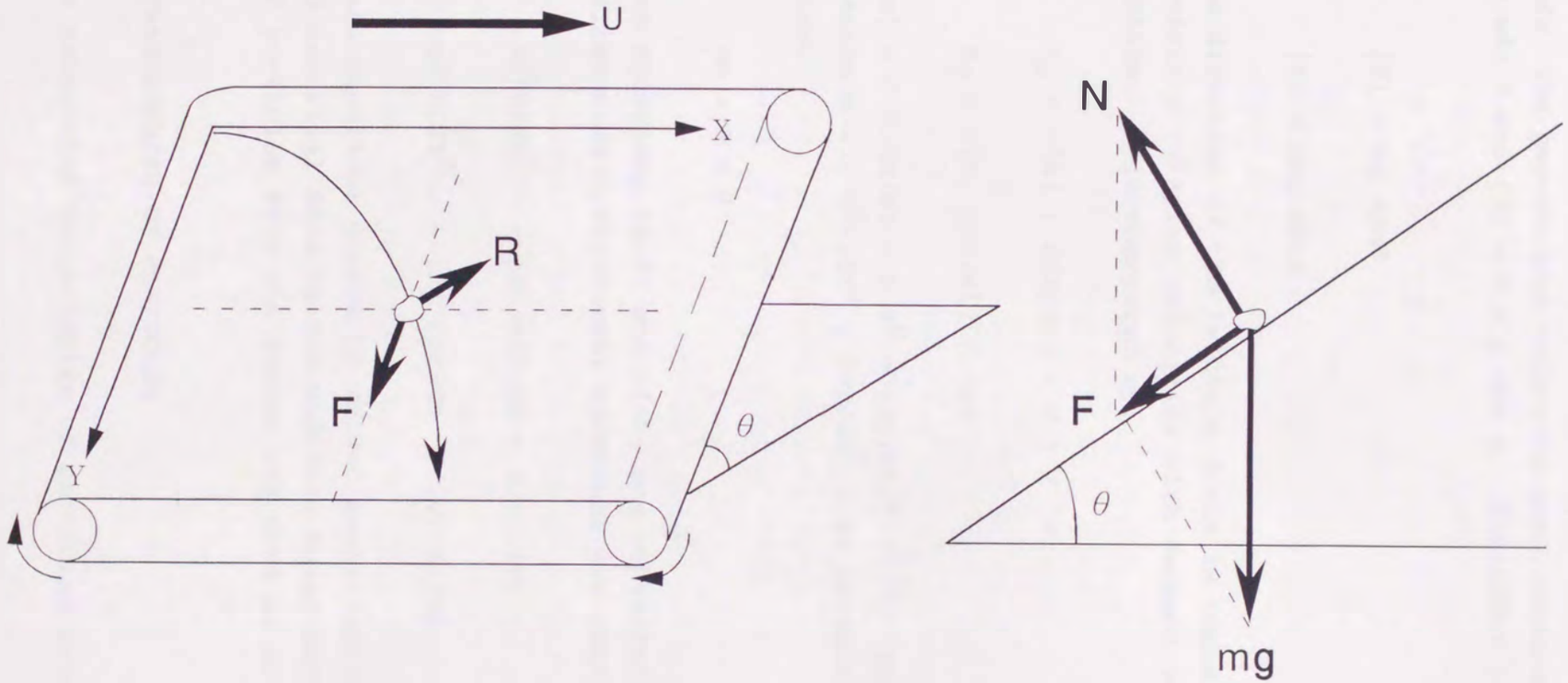


Fig. 4.2 Forces working on a particle on an inclined conveyor

Here, the geometrical relations were obtained in Fig. 4.2 as $F = m\ g \sin\theta$ and $|\mathbf{N}| = \theta\ m\ g \cos\eta$. Equations (4-3) and (4-4) were

$$|\mathbf{F}| = mg \sin\theta \tag{4-5}$$

$$|\mathbf{R}| = \mu mg \cos\theta \tag{4-6}$$

The direction of the friction force is opposite to that of the particle's relative velocities with respect to the inclined moving plate. **R** is expressed by:

$$R_x = -|\mathbf{R}| \left( (dX/dt) - U \right) / |\mathbf{v}| \tag{4-7}$$

$$R_y = -|\mathbf{R}| (dY/dt) / |\mathbf{v}| \tag{4-8}$$

where $|\mathbf{v}| = \left( \left( dx/dt - U \right)^2 + (dy/dt)^2 \right)^{1/2}$. The particle acceleration $\mathbf{a} = \left( d^2x/dt^2 , d^2y/dt^2 \right)$ is calculated by Newton's Second Law:

$$m\mathbf{a} = \mathbf{R} + \mathbf{F} \tag{4-9}$$

When equations (4-7) and (4-8) are substituted into equation (4-9), first rank differential equations are obtained:

$$md^2X/dt^2 = - |\mathbf{R}| (dX/dt - U) / |\mathbf{v}| \tag{4-10}$$

$$md^2Y/dt^2 = - |\mathbf{R}| (dY/dt) / |\mathbf{v}| + |\mathbf{F}| \tag{4-11}$$

These equations cannot be solved analytically; therefore, we obtained numerical data by the modified Euler method. The feed point of particles from the feeder was used as an initial condition.

### 4.2.3 TRAJECTORIES OF PARTICLES

The calculated trajectories of particles from the theoreti-

cal analysis are in Figs. 4.3 - 4.6 where the belt speed and an inclination angle are given. As shown in these figures, it is clear that the trajectories depend on the friction coefficients of the particles. Low-friction particles tend to rapidly roll down, while particles with high friction are transported by the conveyor and thrown out from the right edge.

The effect of the belt moving speed is seen in Figs. 4.3 and 4.4. The difference in the trajectories was not so great. The trajectories dependent on the friction coefficients were slightly closer at the higher belt transportation speed.

It seems that the angle of the inclined conveyor is more important than the belt speed as operating factors as shown in Figs. 4.4 - 4.6. Particles which have greater friction than the tangent of the inclination angle are independent of the conveyor speed and are, therefore, transported by the conveyor. The solid lines in these figures are the trajectories of particles having less friction coefficient than the tangent of the inclination angle, and broken lines indicate larger friction coefficients.

For example, all of the trajectories were able to be close, and particles whose friction coefficients were 0.1 to 0.5 rolled down in the small X displacement when an inclination angle was high such as in Fig. 4.6.

As shown in these figures, a friction angle seems to be very important to illustrate the division of particle trajectories into two domains. Lower friction particles tend to roll down rapidly. The motion of those with a higher friction is independent of the conveyor speed: they are transported by the conveyer and thrown out from the right edge.

The trajectories at different belt speeds and inclination angles were also strongly dependent on the friction coefficient. It became clear that the angle of the inclined conveyer was a more important operating variable than the belt transportation speed.

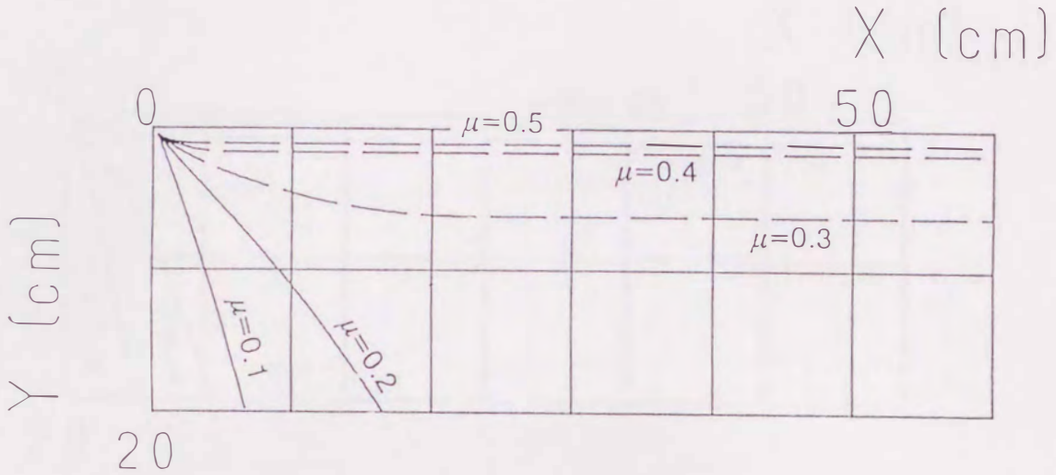


Fig.4.3 Trajectory of particles ; plate width : 20 cm
θ=15° U=0.38 m/s

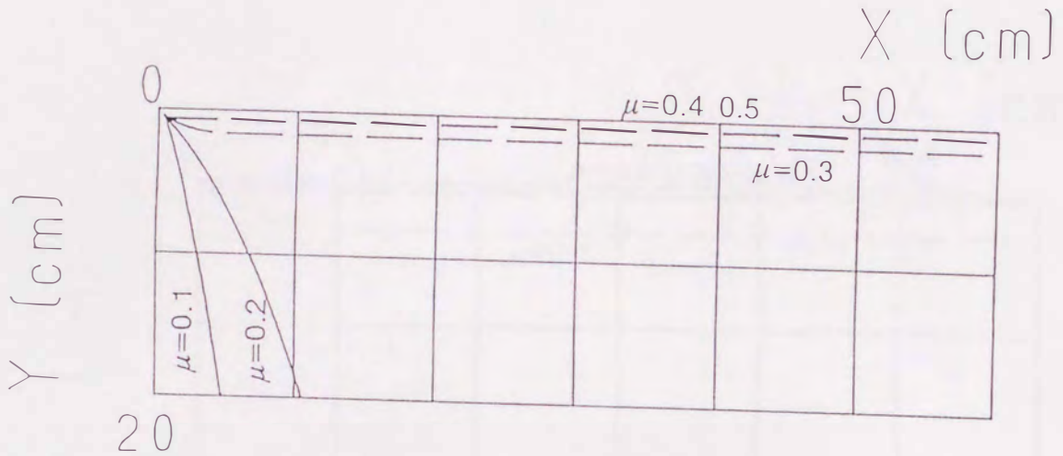


Fig.4.4 Trajectory of particles ; plate width : 20 cm
θ=15° U=0.17 m/s

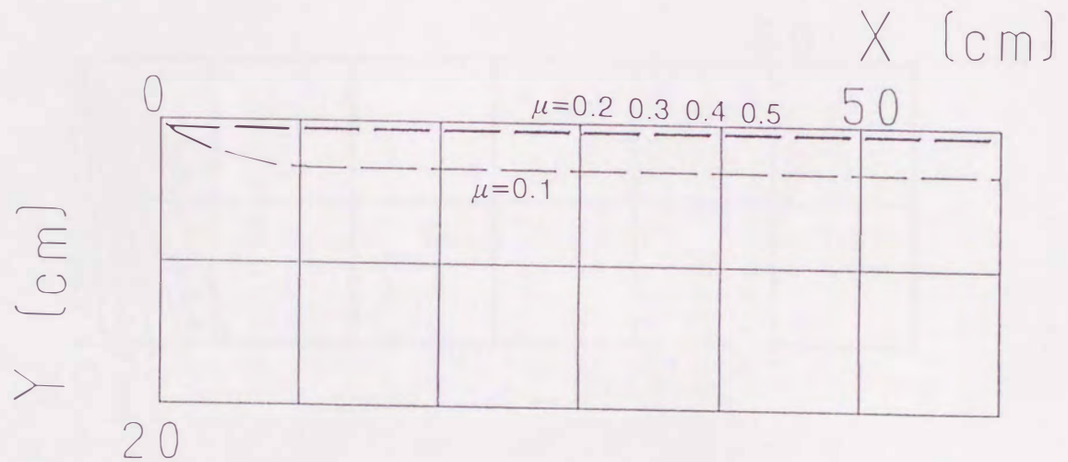


Fig.4.5 Trajectory of particles ; plate width : 20 cm
θ=5° U=0.17 m/s

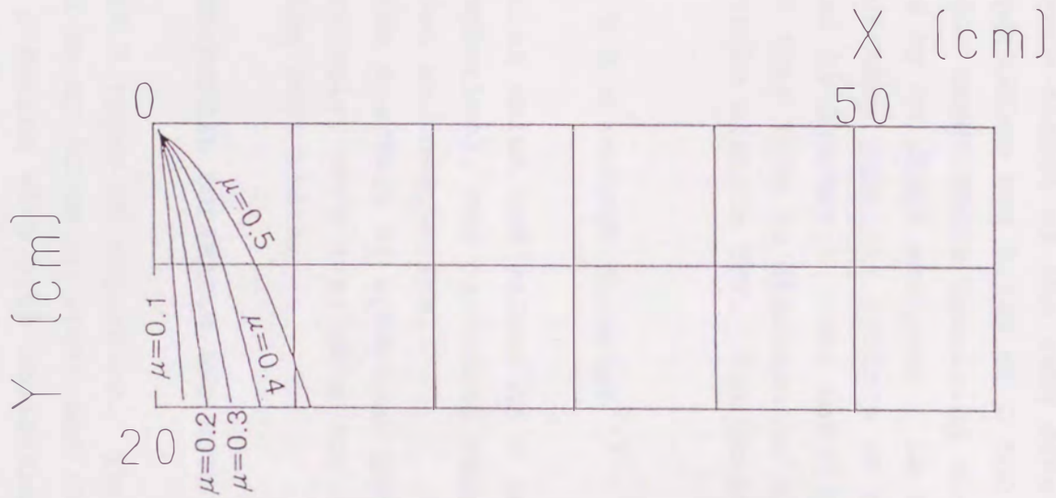


Fig.4.6 Trajectory of particles ; plate width : 20 cm
θ=30° U=0.17 m/s

## 4.3 Comparison of experimentally collected position with calculated trajectory

### 4.3.1 MATERIAL AND ANALYSIS

Kashima sands mixed with glass beads were used as an experimental material. Kashima sands were sieved to obtain sizes from 500-to-850 μm. Glass bead sizes ranged from 500-to-710 μm. The materials were almost of the same density. The mass fraction of spherical particles was 0.249 or 0.500 and, respectively, made available for experiments involving the 20cm or 60cm belt width, as measured by an image analyzer ( LA-555 by PIAS Co., Ltd. ).

We have many possible factors to decide the particle shape as described in Chapter 1. The ratio of diameter and area, ψ, was used at this time to diminish an aberration from pixel density and particle size in CRT. The shape factor, ψ, was calculated as :

$$\psi = ( 0.5 \times \text{maximum diameter} )^2 / \text{project area} \qquad (4\text{-}12)$$

Particles which had values of ψ smaller than 1.2 were regarded as spherical, and particles whose ψ was greater than 1.2 were regarded as nonspherical.

The mass fraction of spherical particles of 0.249 and 0.500 was, respectively, made available for experiments involving the 20cm and 60cm belt width.

### 4.3.2 EXPERIMENTAL APPARATUS AND METHOD

We used 2 types of apparatus. The belt of the inclined conveyor is 20 cm or 60 cm in width and 100 cm in length. The belt is made of plastics with high resistance against electrostatic charging. This conveyor is driven with velocity U by a roller.

The inclination angle can be varied from 0 to 90°. The particles were collected in vessels 1-8 or 1-7 located as illustrated in Figs. 4.7 and 4.8.

The belt speed varied from 0.038 m/s to 0.583 m/s, and an

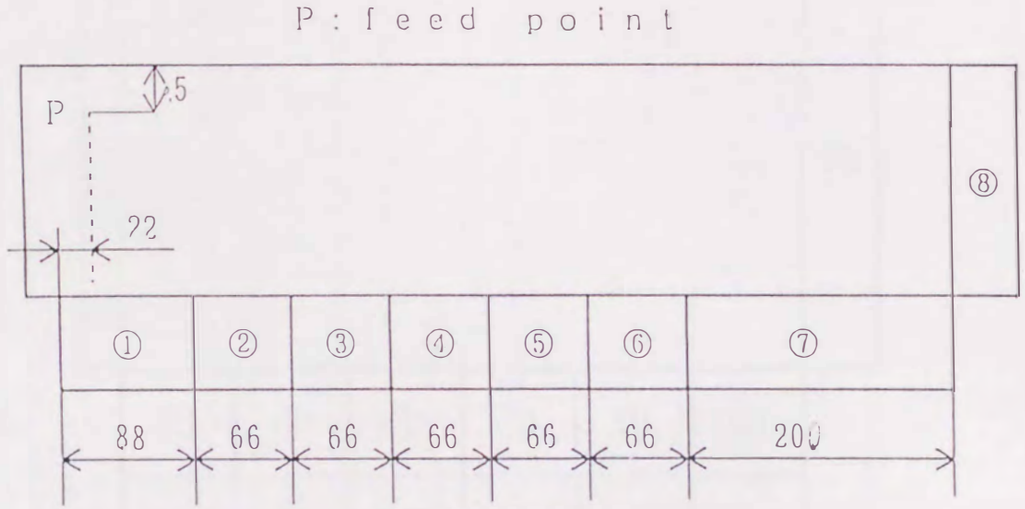


Fig.4.7 Positions of the feed point and vessels on the 200 mm wide belt
(dimension is mm)

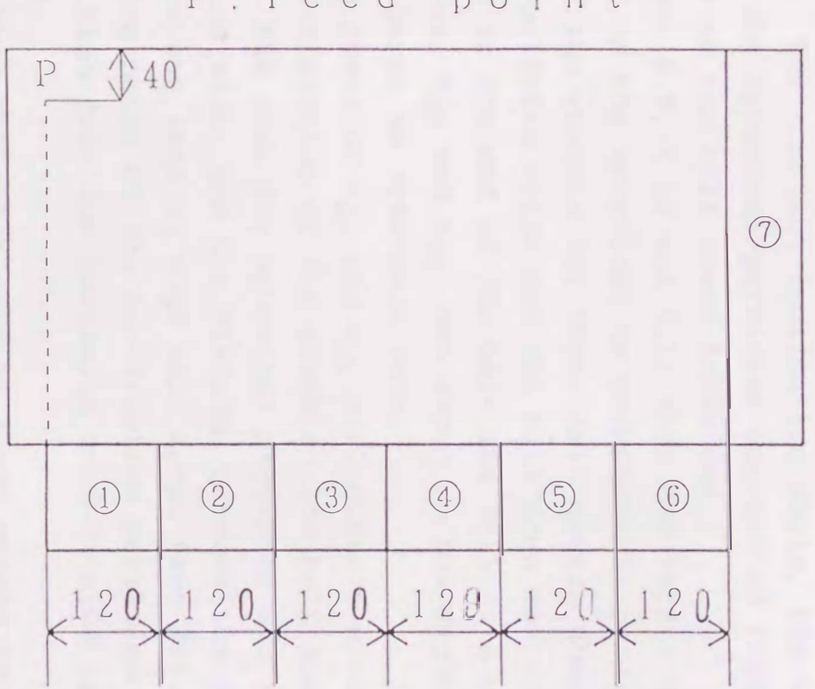


Fig.4.8 Positions of the feed point and vessels on the 600 mm wide belt
(dimention is mm)

inclination angle was 5, 15 or 30°. The experimental material was fed at point P on the belt with a small tube. The feed rate was small enough to neglect the interaction of the particles. The collected particles in the vessels were weighed, and the mass fraction of each was measured using an image analyzer.

Recoveries of spherical and nonspherical particles in the respective vessels were calculated by the equations in the Appendix.

### 4.3.3 EFFECT OF BELT SPEED[54]

Belt speed and inclination angle were important operating factors. For constant inclination angle, the theoretical trajectory of the spherical particles approached that of the nonspherical ones as the belt speed increased.

Figs. 4.9, 4.10 and 4.11 show the relationship between the recovery of the spherical or nonspherical particles and the positions of the vessels for three belt speeds when the belt was 20cm wide. Particles which did not roll down to vessels 1-7 were conveyed to the end of the belt and fell into vessel 8. The recoveries, $r_{S8}$ and $r_{N8}$, are shown in the right hand side of these figures as reference data.

The peaks of $r_{Si}$ and $r_{Ni}$ were clearly divided to both sides in the X-direction of the graph at low belt speed (see Fig. 4.9). However, the peak for spherical particles was shifted to the right hand side, and the distance between the two peaks in the X-direction was less at high belt speed (see Fig. 4.11), because the trajectories of the low-friction particles approached those for the high-friction particles as indicated in the theoretical analysis.

Another characteristic of these graphs is that the peak of the spherical particles became broad at high belt speed. This agreed with the results by the calculated trajectories in the theoretical analysis.

### 4.3.4 EFFECT OF INCLINATION ANGLE[54]

The inclination angle is more important as an operating

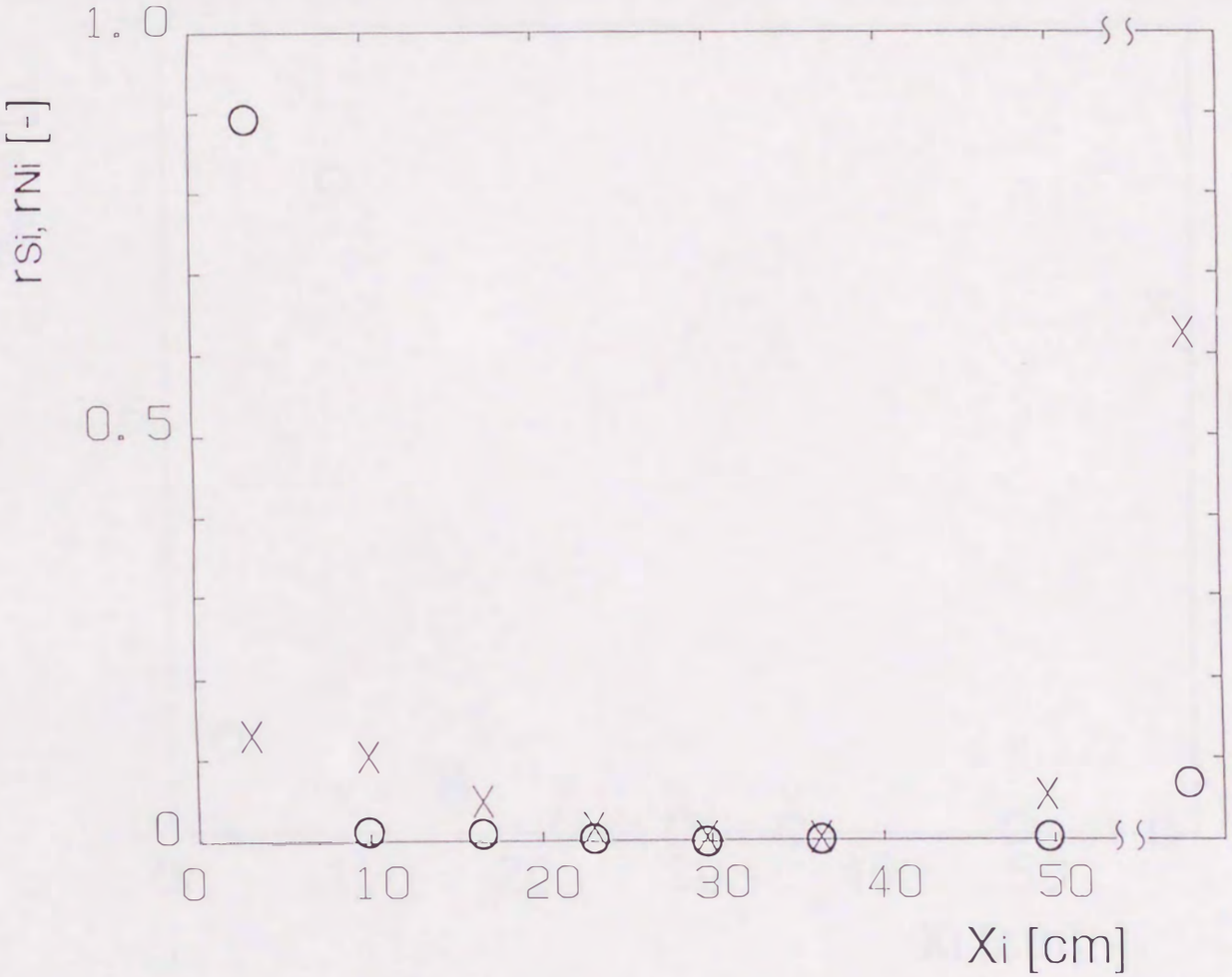


Fig.4.9 Effect of the position of a recovery vessel on the recovery of particles o sphere x nonsphere
U : 0.038 m/s $\theta$ : 15° belt width : 20 cm

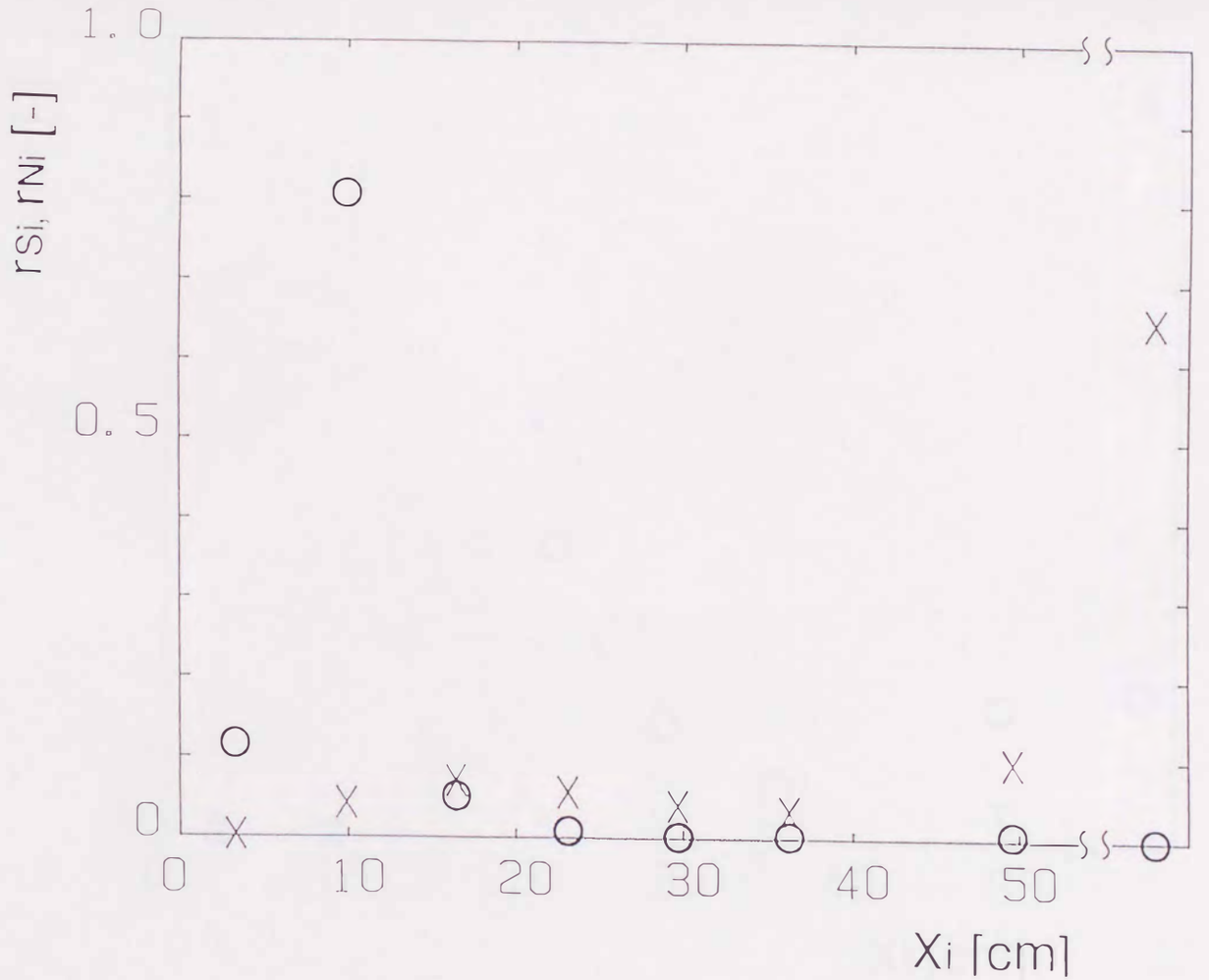


Fig.4.10 Effect of the position of a recovery vessel on the recovery of particles o sphere x nonsphere
U : 0.172 m/s $\theta$ : 15° belt width : 20 cm

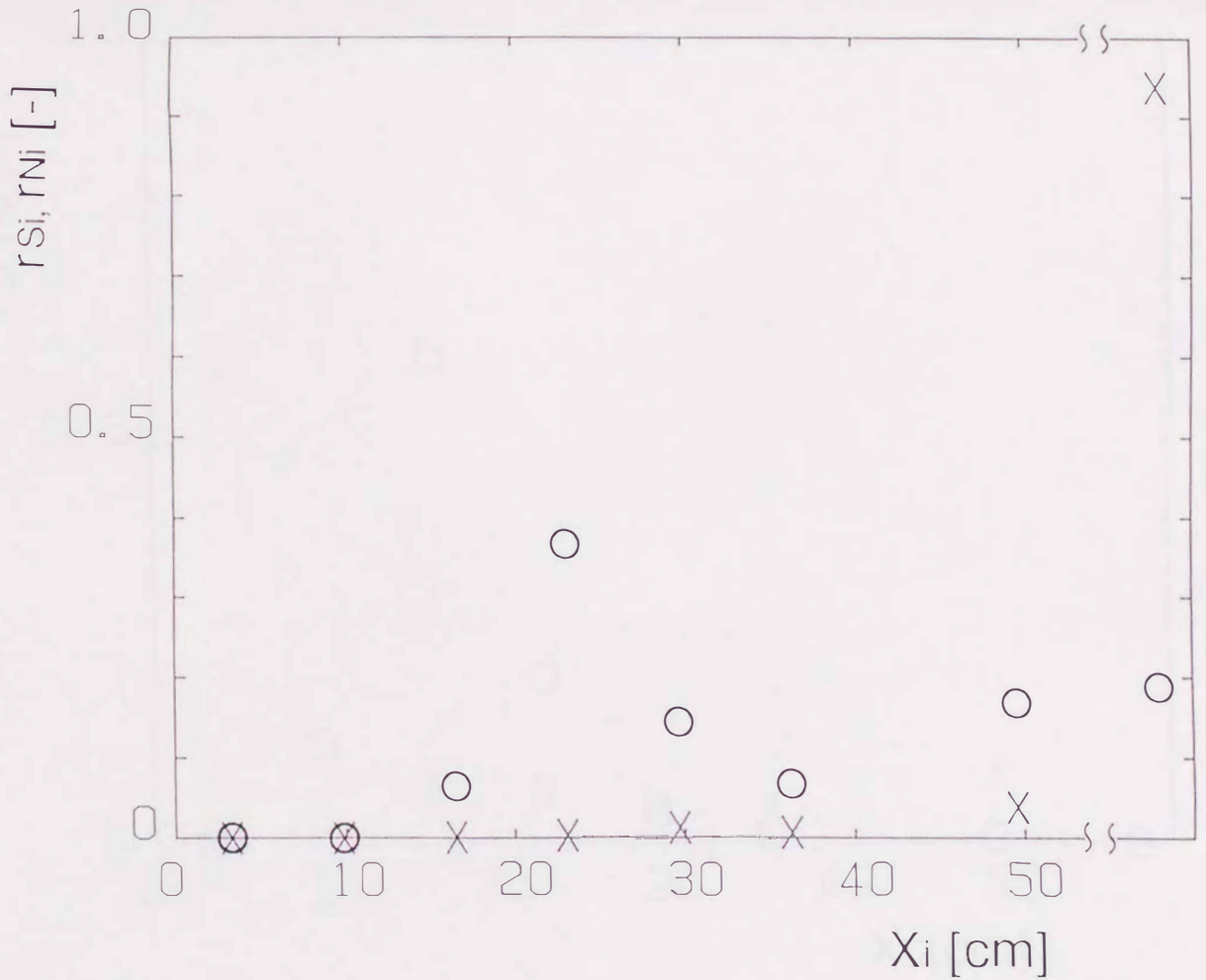


Fig.4.11 Effect of the position of a recovery vessel on the recovery of particles o sphere x nonsphere
U : 0.375 m/s $\theta$ : 15° belt width : 20 cm

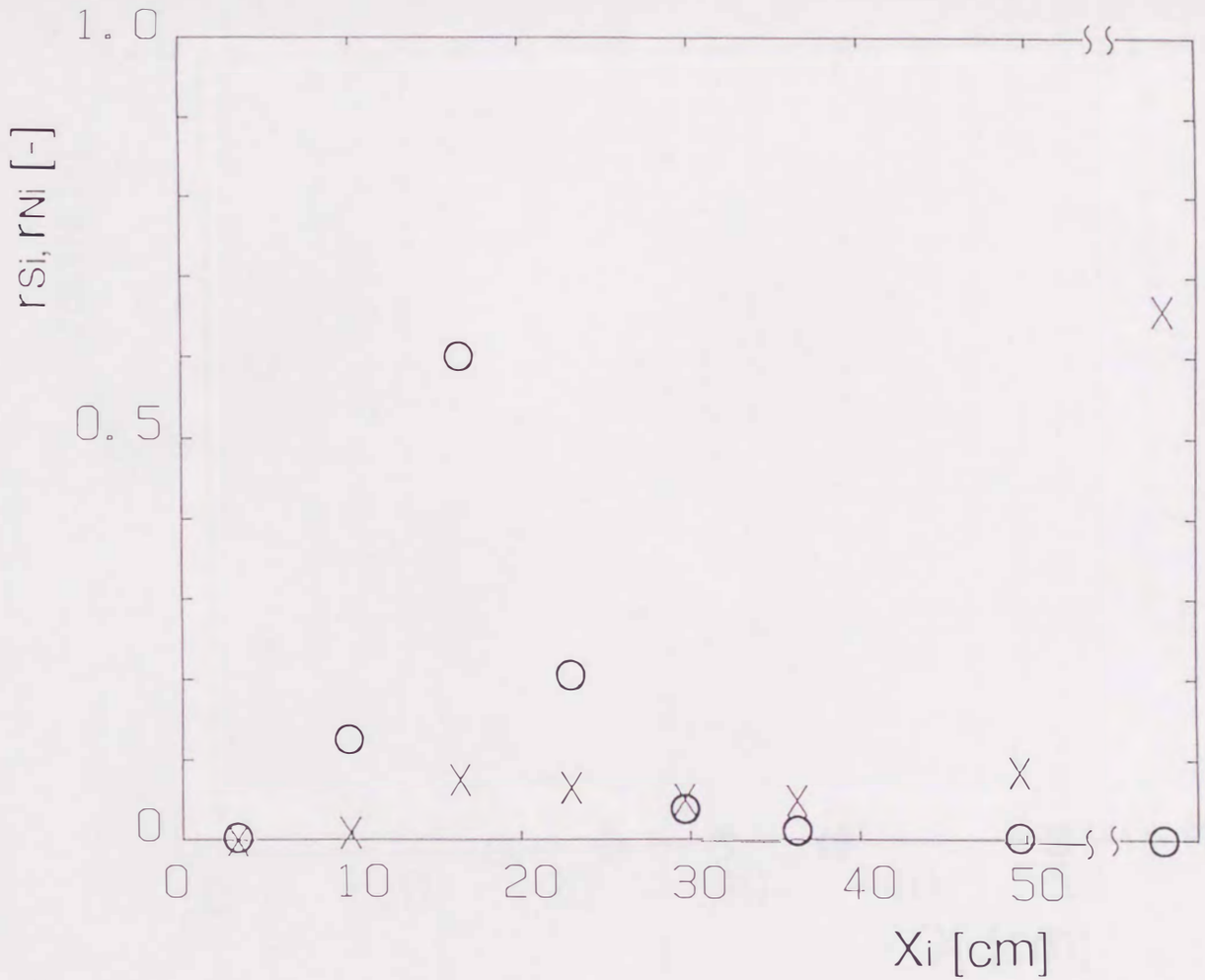


Fig.4.12 Effect of the position of a recovery vessel on the recovery of particles o sphere x nonsphere
U : 0.167 m/s $\theta$ : 5° belt width : 20 cm

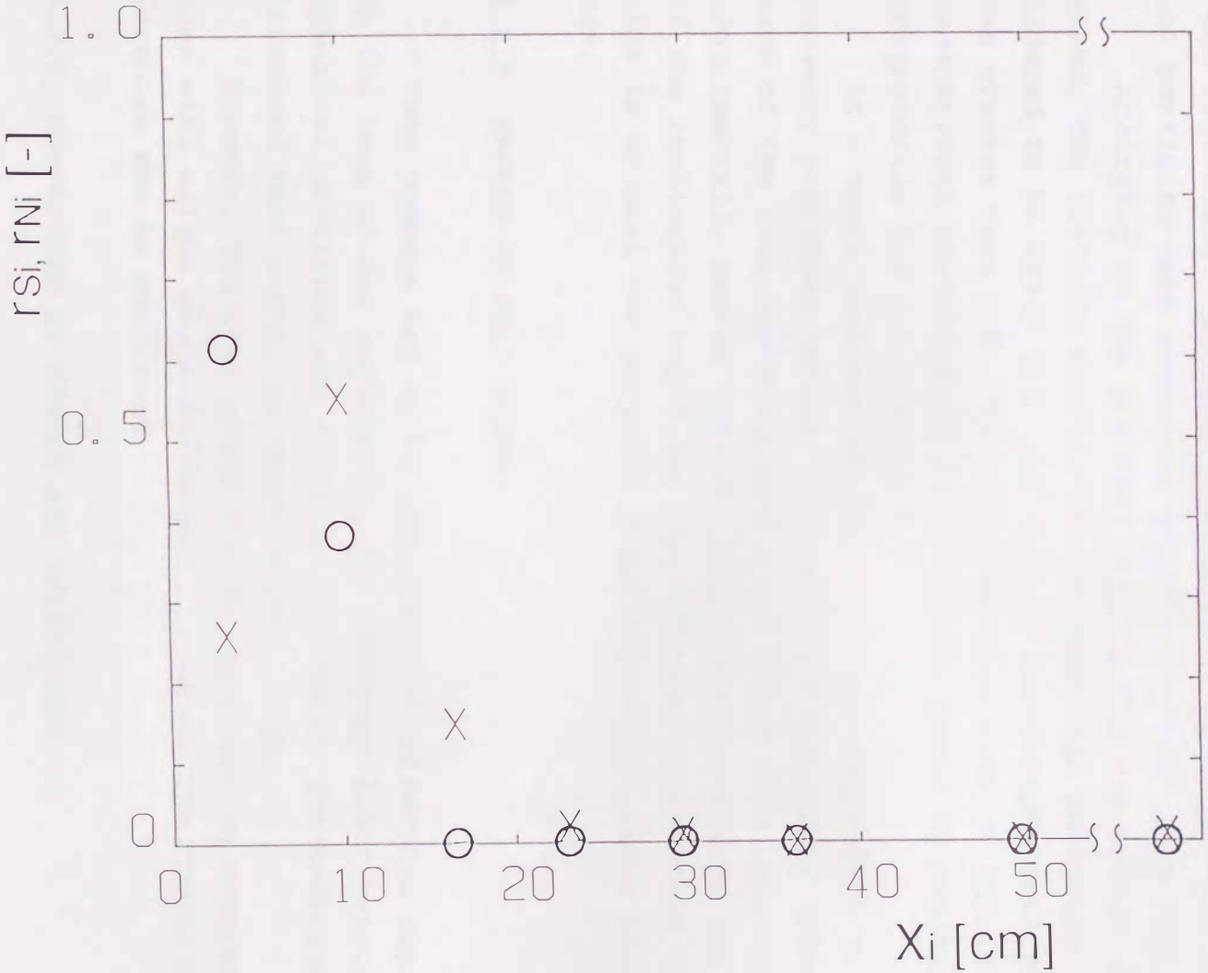


Fig.4.13 Effect of the position of a recovery vessel on the recovery of particles o sphere x nonsphere
U : 0.170 m/s $\theta$ : 30° belt width : 20 cm

condition than belt speed, as pointed out earlier in this thesis. Figs. 4.10, 4.12 and 4.13 show the experimental results confirming this prediction.

The recovery distribution of nonspherical particles almost overlapped that of the spherical particles at 30° inclination (see Fig. 4.13). However, the peaks of spherical and nonspherical particles were obviously separated at 15° (see Fig. 4.10).

According to the previous results for the effect on belt speed, the friction coefficient of spherical particles was considered to be about 0.2, and that of the nonspherical particles was greater than 0.3. The recovery positions of spherical and nonspherical particles in these figures could be explained by trajectories for $\mu$ = 0.2 and 0.5.

At a small inclination angle, it was impossible to predict recovery positions because they were conspicuously affected by a warp of the belt and a slight vibration in this apparatus. It is experimentally proved that the relationship between the tangent of the inclination angle and the friction coefficient of particles is crucial for particle shape separation using this apparatus.

### 4.3.5 EFFECT OF BELT WIDTH

This appears not to be important for effective separation. In the case of our experiment, the recovery distribution of spherical particles was slightly shifted in the X-direction for increased belt width, as shown in Fig. 4.14.

However, the belt width may be important to separate particles with slight shape differences, because the trajectory differences can be amplified.

### 4.3.6 COMPARISON OF THEORY AND EXPERIMENT[54]

Figs. 4.15, 4.16 and 4.17 show the effect of the inclination angle and belt speed on particle friction. The lines in the graphs represent the theoretical curves for the friction coefficient values of 0.2 and 0.5. The experimental results are expressed by the short segments, which are in the range for 60% of

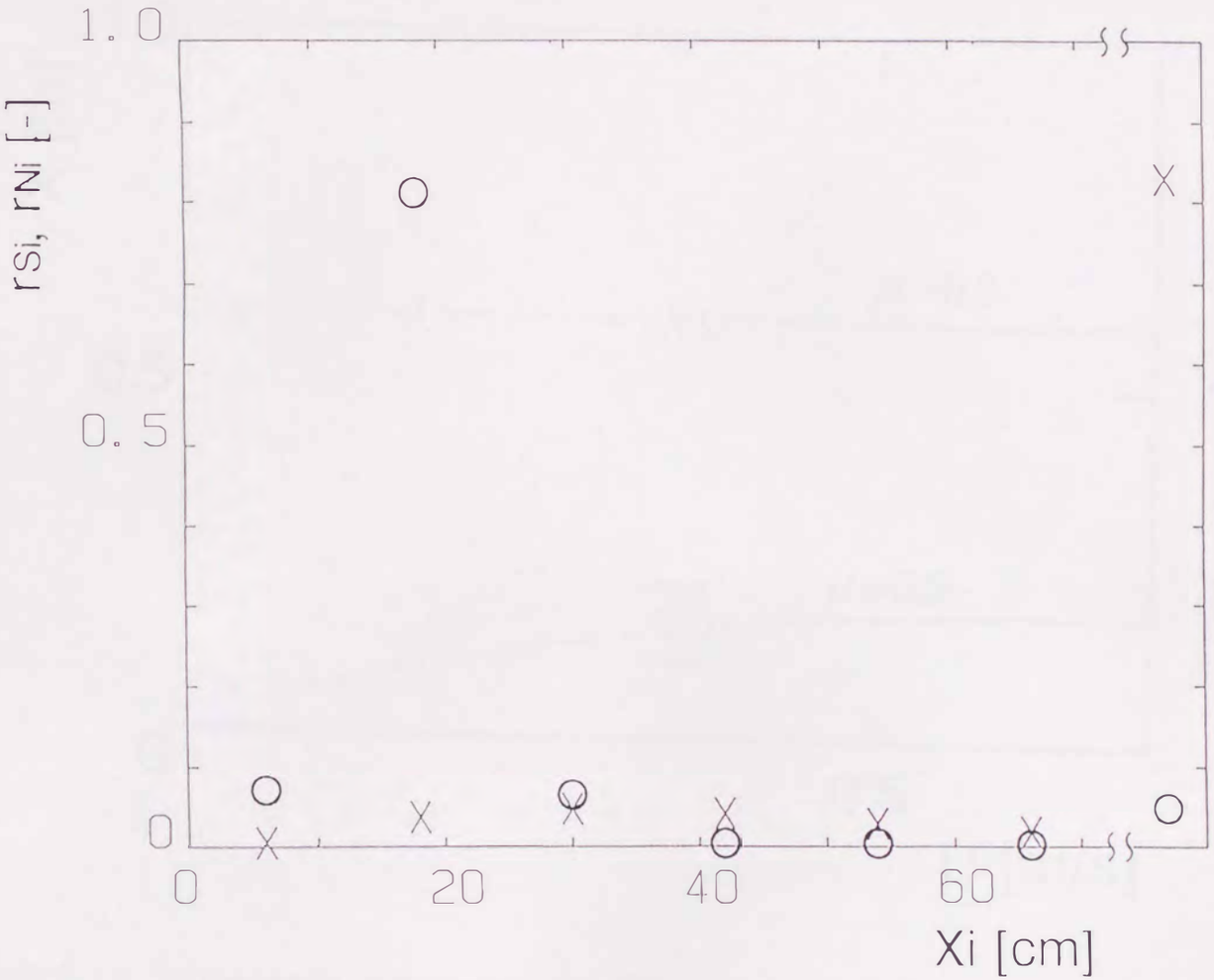


Fig.4.14 Effect of the position of a recovery vessel on the recovery of particles o sphere x nonsphere
U : 0.167 m/s $\theta$ : 15° belt width : 60 cm

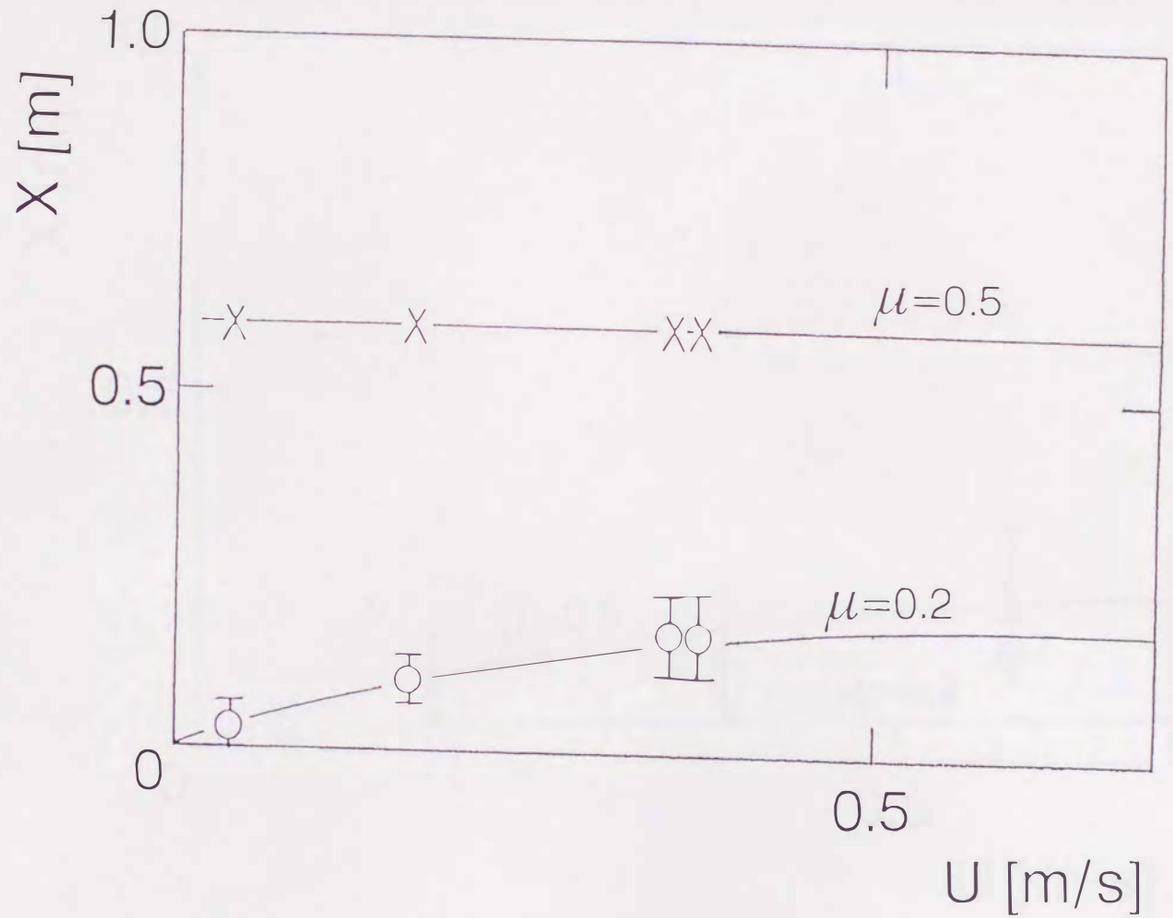


Fig.4.15 Relationship between recovery positions of particles and belt speed o sphere x nonsphere
$\theta$ : 15° belt width : 20 cm

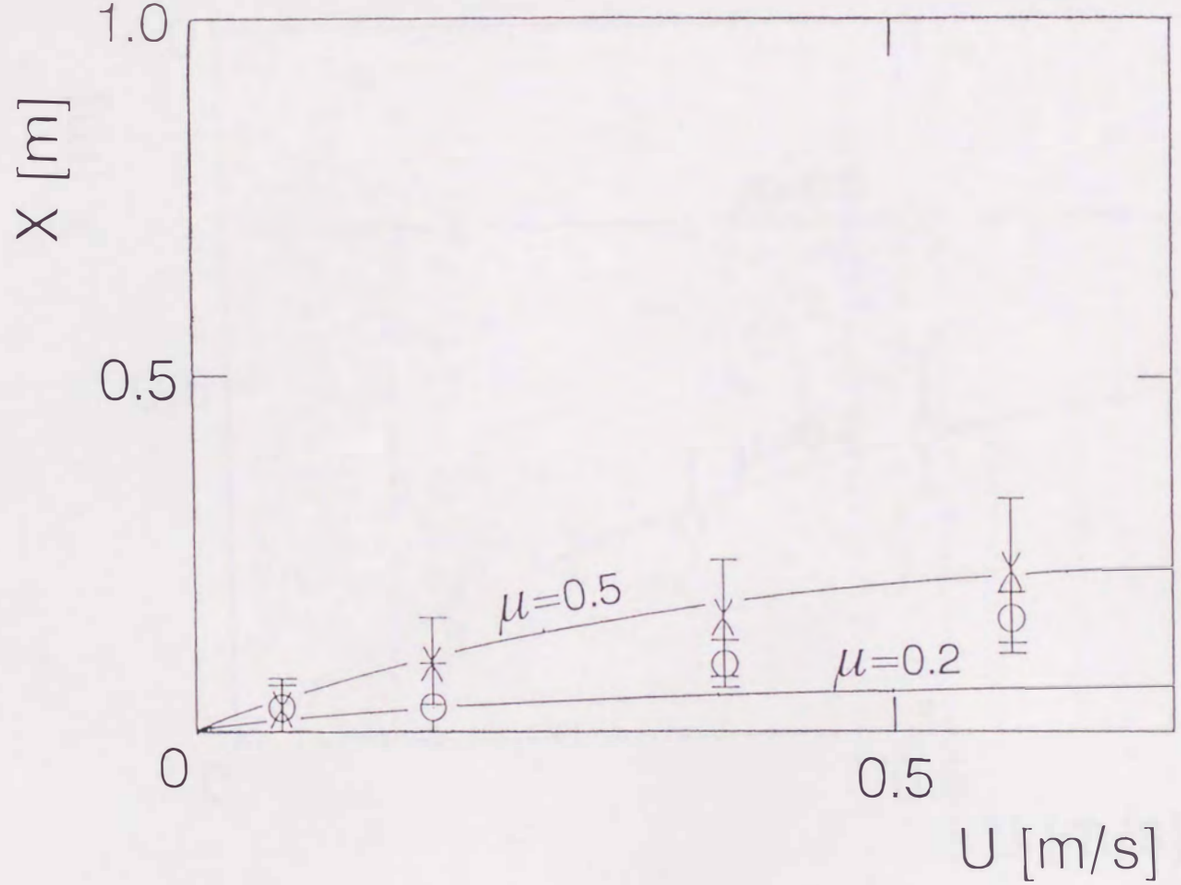


Fig.4.16 Relationship between recovery positions of particles and belt speed o sphere x nonsphere
$\theta$ : 30° belt width : 20 cm

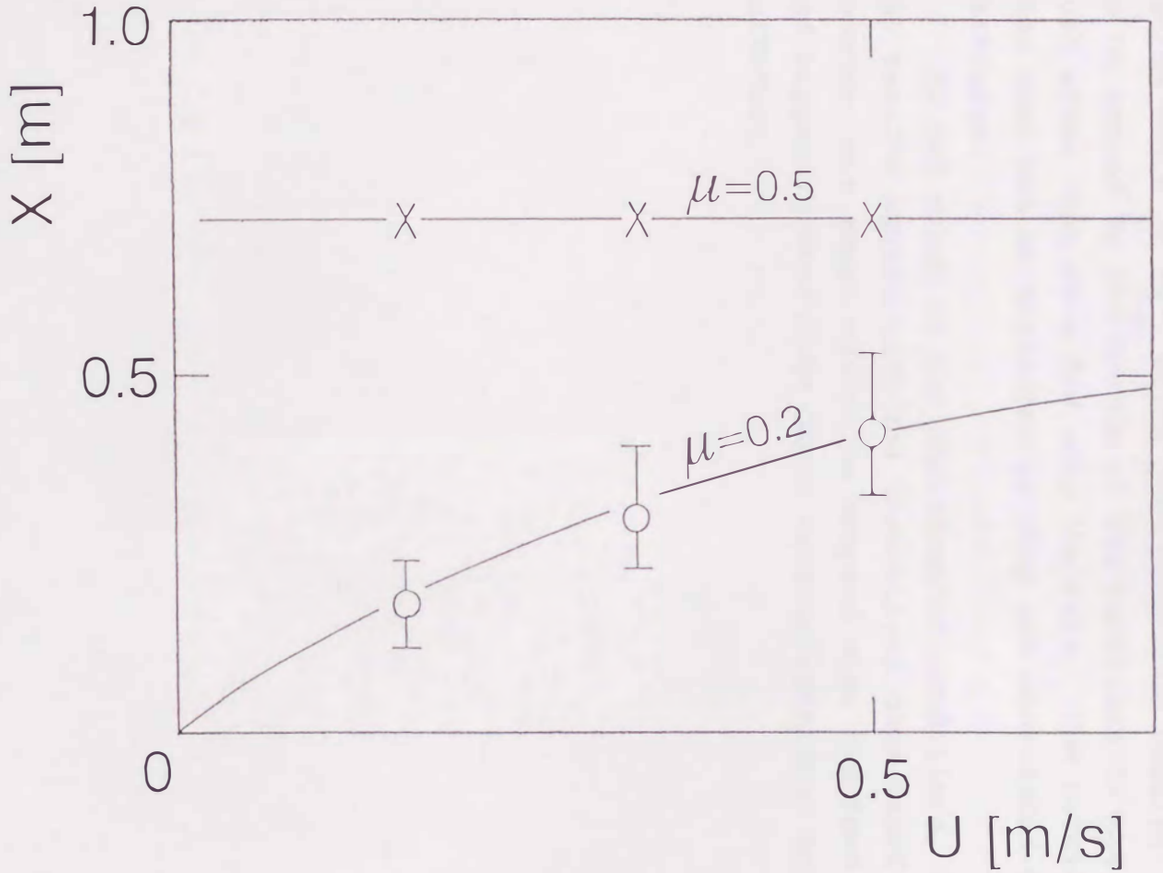


Fig.4.17 Relationship between recovery positions of particles and belt speed o sphere x nonsphere
$\theta$ : 15° belt width : 60 cm

the spherical and non-spherical particles recovered. The results at different inclination angle and belt width agreed with theoretical trajectories.

It would be decided that the friction coefficient of the spherical particles was about 0.2 and that of the nonspherical particles was about 0.5, except for high belt speed and an inclination angle of 30°, which gave anomalous results. This seemed to be caused by the bounce of the particles in the x-direction just after they were fed onto the belt. The rotation of particles must not be neglected as they are considered to be material particles.

In the range of our experimental conditions, the experimental results agreed with the theoretical ones based on our model. However, our model cannot be adopted when the feed rate increases and bigger interactions occur between spherical and nonspherical particles.

## 4.4 Conclusions

The inclined conveyor was introduced in this chapter. The transported force of the particles is worked by the moving belt. The trajectories of spherical and nonspherical particles could be calculated.

The effects of the belt speed, inclination angle and belt width for the separation were experimentally investigated. The inclination angle was the most important operating condition and its tangent value should be intermediate between the friction coefficient of spherical and nonspherical particles.

We could compare the experimental result with the theoretical trajectories of the particles. The friction coefficient of spherical and nonspherical particles would be 0.2 and 0.5 respectively.

# Chapter 5. RECOVERY OF RECLAIMED FOUNDRY SANDS WITH INCLINED CONVEYOR

## 5.1 Introduction

Some of the researchers tried to apply the particle shape separation to industry[55-57].

The treatment of large amounts of materials is necessary in industrial processing. This apparatus has the advantage of conveying particles by the motion of belt. It is faster than the other apparatus.

We tried to add an additional idea to treat a larger amount of materials. Scale-up merit was not important as described in section 4.3.3. However, the trajectories of spherical and non-spherical particles were sharply divided under good experimental conditions.

Materials were fed in the line instead of the point to increase the amount of treatment. The angle of the feed line is important to avoid an interruption of each trajectory.

Reclaimed foundry sand was used as experimental material as shown in Fig. 5.1. The spherical particles are Cerabeads (Naigai Cerabeads by Naigai Ceramics Co., Ltd.), which have excellent properties to make a complicated foundry mold. They are really easy to handle because of their round shape. The Cerabeads were newly developed ceramic mullite beads to be used as foundry sand. The irregular particles are silica sands, a traditional foundry sand.

The characteristics of reclaimed foundry sands are in Table 5.1. The size range and density are about the same. They can be used only in the same manner as traditional foundry sands. When the Cerabeads can be recovered by use of particle shape separation, it is very good business for an industrial foundry.

It is a very good application of the particle shape separation technique. It was carried out as a cooperative project with Eriez Magnetics Japan Co., Ltd.

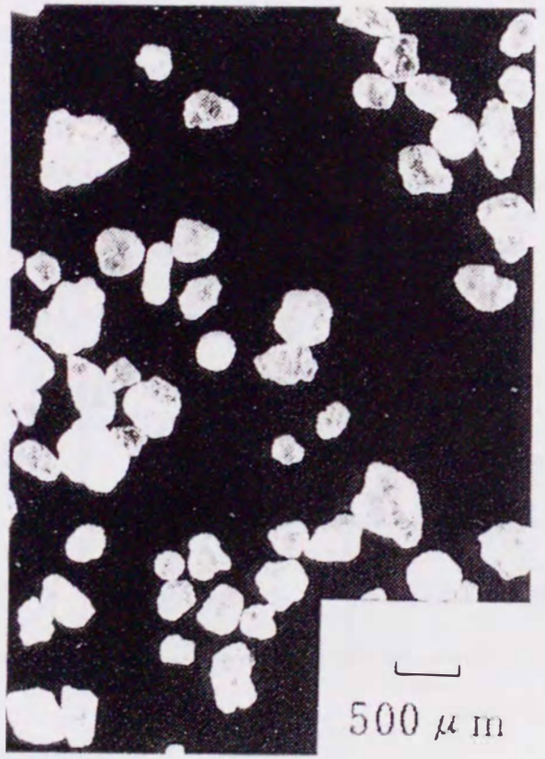


Silica sand

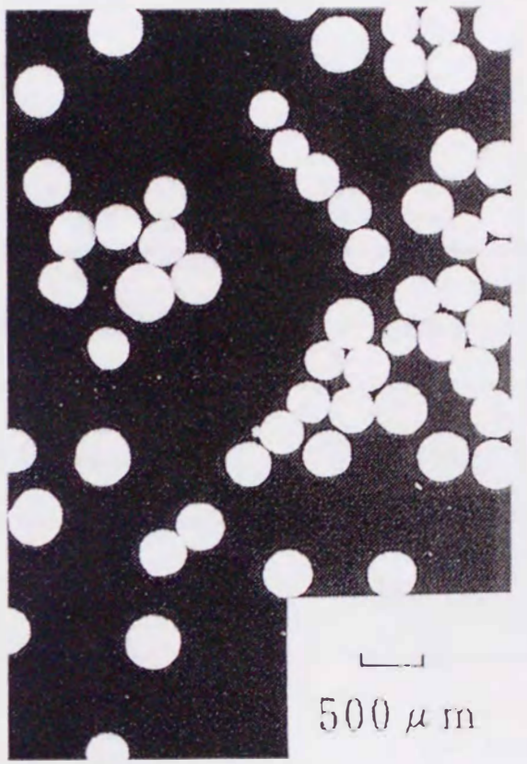


Cerabeads

Fig.5.1 Photograph of reclaimed foundry sands
(mixture of silica sands and cerabeads)

Table 5.1 Content of reclaimed foundry sand

| | Shape | Size Range | Mean Diameter | Density |
|---|---|---|---|---|
| Silica Sands | irregular | 0.1 - 0.5 mm | 0.207 mm | 2.65g / $cm^3$ |
| Cerabeads | spherical | 0.3 - 0.5 mm | 0.362 mm | 2.89g / $cm^3$ |

## 5.2 Separation and recovery performance of advanced foundry sands

### 5.2.1 EXPERIMENTAL APPARATUS AND METHOD

The inclined conveyor, which has a 20cm-wide and 100cm-long belt as shown in Fig. 4.1, was used to recover artificial ceramic beads from reclaimed foundry sands.

The foundry sands were mixtures of ceramic mullite beads called Cerabeads and sillica sands, which were obtained from Eriez Magnetics Japan Co., Ltd. The mass fraction of Cerabeads in reclaimed foundry sands was 0.527 by measurement with an image analyzer.

For this experiment, the belt speed and the angle of inclination were fixed at 0.50 m/s and 20° based on the results of theoretical analysis. Reclaimed foundry sand was fed to point P by a vibrating feeder with a V-shaped trough and collected in vessels 1-8 located in positions as illustrated in Fig. 4.7. The particles collected in the respective vessels were weighed, and their mass fractions in each collected particle were measured by the photographic survey.

### 5.2.2 LIMIT OF TREATMENT CAPACITY[58]

Table 4.2 shows the results of the separation performance at two different feed rates, $W_F$. The recovery of spherical particles ( Cerabeads ) in the product, $r_{SP}$, recovery of nonspherical particles ( Silica Sand ) in the residue, $r_{NR}$, and Newton's separation efficiency, $\eta$, were calculated by the equations in the Appendix.

The maximum value of $\eta$ is presented in Table 4.2 where the dividing point between product and residue was appropriately decided.

The inclination angle, $\theta$, and belt speed, U, were important operating conditions as pointed out in the last chapter. However, under constant operation, separation efficiency decreased as

Table 5.2 Recovery and separation efficiency of reclaimed foundry sand

| Feed Rate $W_F$ | Recovery of Spherical Particles $r_{SP}$ | Recouvery of Nonspherical Particles $r_{NR}$ | Newton`s Separation Efficiency $\eta$ |
|---|---|---|---|
| 0.250 g/s | 0.849 | 0.803 | 0.697 |
| 2.42 g/s | 0.999 | 0.579 | 0.578 |

the feed rate increased. It is thought to be caused by the interaction between the Cerabeads and Silica sands.

Fig. 5.2 shows the relationship between the recovery of spherical or nonspherical particles and the positions of the vessels for five different feed rates. The values $X_i$, $r_{Si}$ and $r_{Ni}$ have the same meaning as in Figs. 4.9 - 4.13.

As shown in this figure, the recovery distribution of nonspherical particles was independent of the feed rate within the range of our experimental conditions. When the feed rate was increased, the recovery distribution of spherical particles was shifted to the direction of the belt transportation because the retention of nonspherical particles affected the motion of the spherical particles.

In other words, the theoretical movement of spherical particles was intercepted by nonspherical particles which were conveyed to the end of the belt conveyor, and the spheres tended to be transferred in the X-direction with the nonspheres retained on the belt.

When the feed rate was 0.250 g/s, the separation was fairly good in this case. However, the recovery distributions of spherical particles and nonspherical particles have the same tendency, except for the last recoveries, $r_{S8}$ and $r_{N8}$, at a greater than 1.75 g/s feed rate.

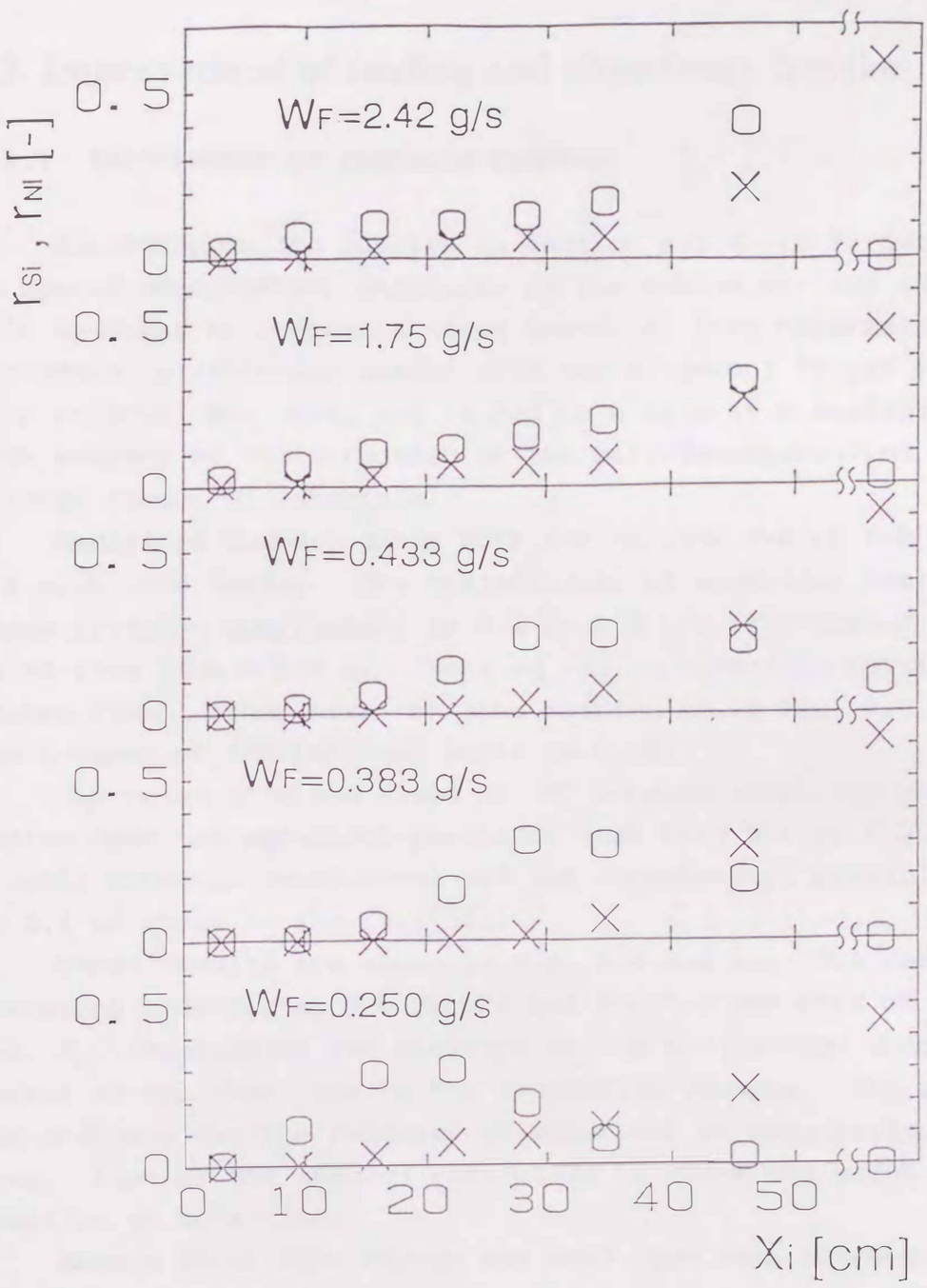


Fig.5.2 Effect of positions of recovered vessels on spherical and nonspherical particles recovery in the vessel
o sphere x nonsphere

## 5.3 Improvement of feeding and abundance fraction

### 5.3.1 IMPROVEMENT OF PARTICLE FEEDING

According to the results in section 5.2.2, it is necessary to spread nonspherical particles on the entire surface of the belt in order to process a large amount of feed materials. Therefore, a vibrating feeder with two different trough widths, 10cm or 30cm, was used, and it fed in a line at $\alpha$ inclination with respect to the direction of the belt transportation to treat a large amount of materials.

Reclaimed foundry sands were fed on line P-A or P-B in Fig. 5.3 with this feeder. The trajectories of spherical particles whose friction coefficient is 0.1 or 0.2 are illustrated by a solid line from P and B. Those of the nonspherical particles are broken lines. They have the same meaning as in Fig. 4.3, because the tangent of the inclined angle is 0.364.

The value of $\alpha$ was fixed at 24° because there was no interaction when the spherical particles must have 0.1 to 0.2 of the kinetic friction coefficient and the nonspherical particles 0.3 to 0.4 as shown in Fig. 5.3[54].

These results are shown in Fig. 5.4 and Fig. 5.5 under the operating conditions, U=0.33 m/s and $\theta$=15°. The axis of abscissas, $X_i$, represented the distance in the x-direction from the center of the feed line to the respective vessels. The axis of the ordinate was the recovery of spherical or nonspherical particles. Some of the samples were mixed to check the weight and fraction at this time.

When a 10 or 30cm trough was used, the same tendency as with the V-type trough was obtained. The recovery distribution of spherical particles was affected by the position of the nonspherical particles when the feed rate was large. A larger amount of feed materials could be processed using line feeding. More than ten times of the feed materials could be processed with a 30cm trough[58].

We succeeded in spreading the nonspherical particles on the wider area of the belt and treated a greater amount of reclaimed

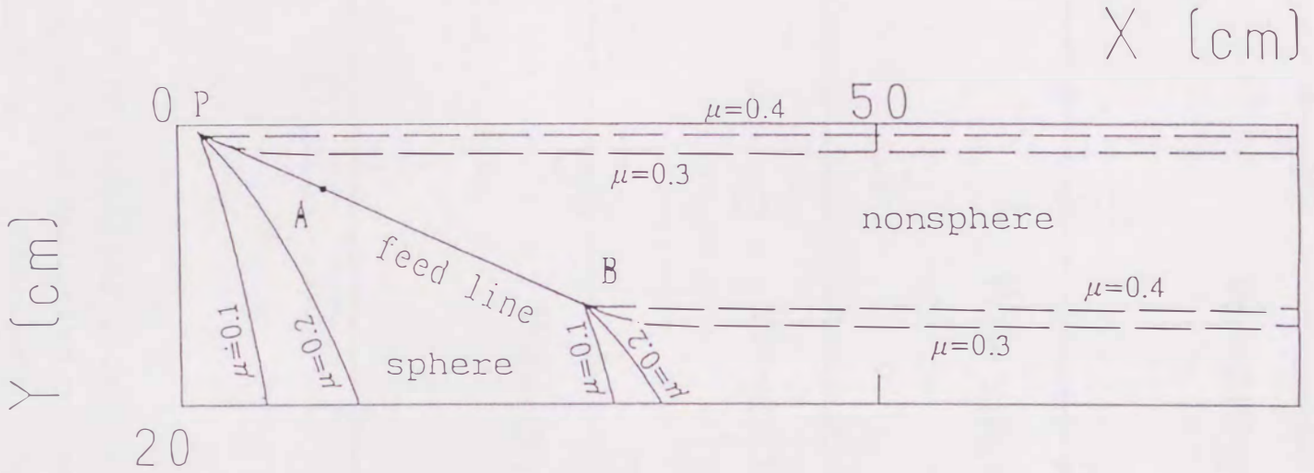


Fig.5.3 Position of feed line and trajectories of particles
$\theta$ = 15° U = 0.33 m/s

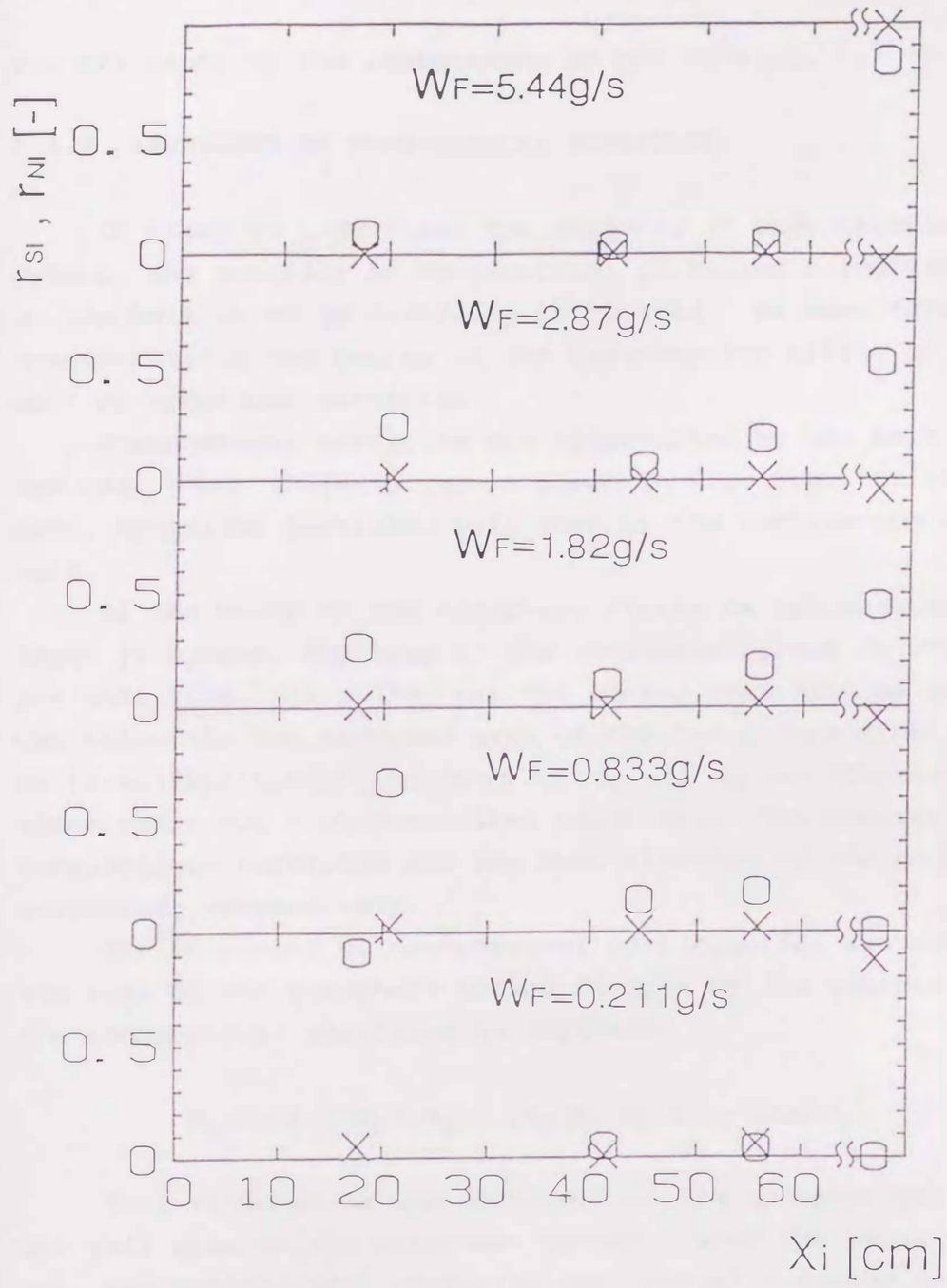


Fig.5.4 Effect of positions of recovered vessels on spherical and nonspherical particles recovery in the vessel
o sphere x nonsphere feed line : 10 cm

foundry sands by the improvement of the feeding.

### 5.3.2 ABUNDANCE OF NONSPHERICAL PARTICLES

In order to understand the capacity of this experimental method, the quantity of nonspherical particles being transported on the belt is to be carefully calculated. We have taken into considerations the degree of its interceptive effect on the movement of spherical particles.

Nonspherical particles are transported by the belt movement and keep their trajectories as shown in Fig. 5.6. On the other hand, spherical particles roll down by the inclination of the belt.

If the width of the nonsphere stream is not changed and the layer is single, the area of the nonsphere spread is $U*l_F*\sin \alpha_l$ per unit time. $(1-x_F)*W_F$ was fed during that time as weight. We can calculate the occupied area of the fed nonspherical particle as $(1-x_F)*W_F/(\varepsilon_N*\rho_N*d_N)$, where $\varepsilon_N$, $\rho_N$ and $d_N$ are the occupied space ratio for a circumscribed hexahedron, the density of the nonspherical particles and the mean diameter of the nonspherical particles, respectively.

The abundance of nonspherical particles[58] was obtained as the area of the nonsphere spread divided by the occupied area of the nonspherical particles as follows:

$$\phi_N = (1 - x_F)\ W_F\ /\ (\varepsilon_N\ \rho_N\ d_N\ U\ l_F\ \sin \alpha_l) \qquad (5\text{-}1)$$

This value means the abundance of the nonspherical particles per unit area on the nonsphere spread. When the value becomes one, the nonspherical particles are virtually packed on the belt without void. In this case, the mass of the nonspherical particles in the unit volume on the belt is the same as the density multiplied space ratio of the nonspherical particles. When the value is 0, there are no nonspherical particles on the belt.

Fig. 5.7 indicates the relationship between $X_i$ and the recovery when the abundance of nonspherical particles is almost the same, but different trough widths were used. The upper graph is for the 10cm trough, and the lower graph is for the 30cm

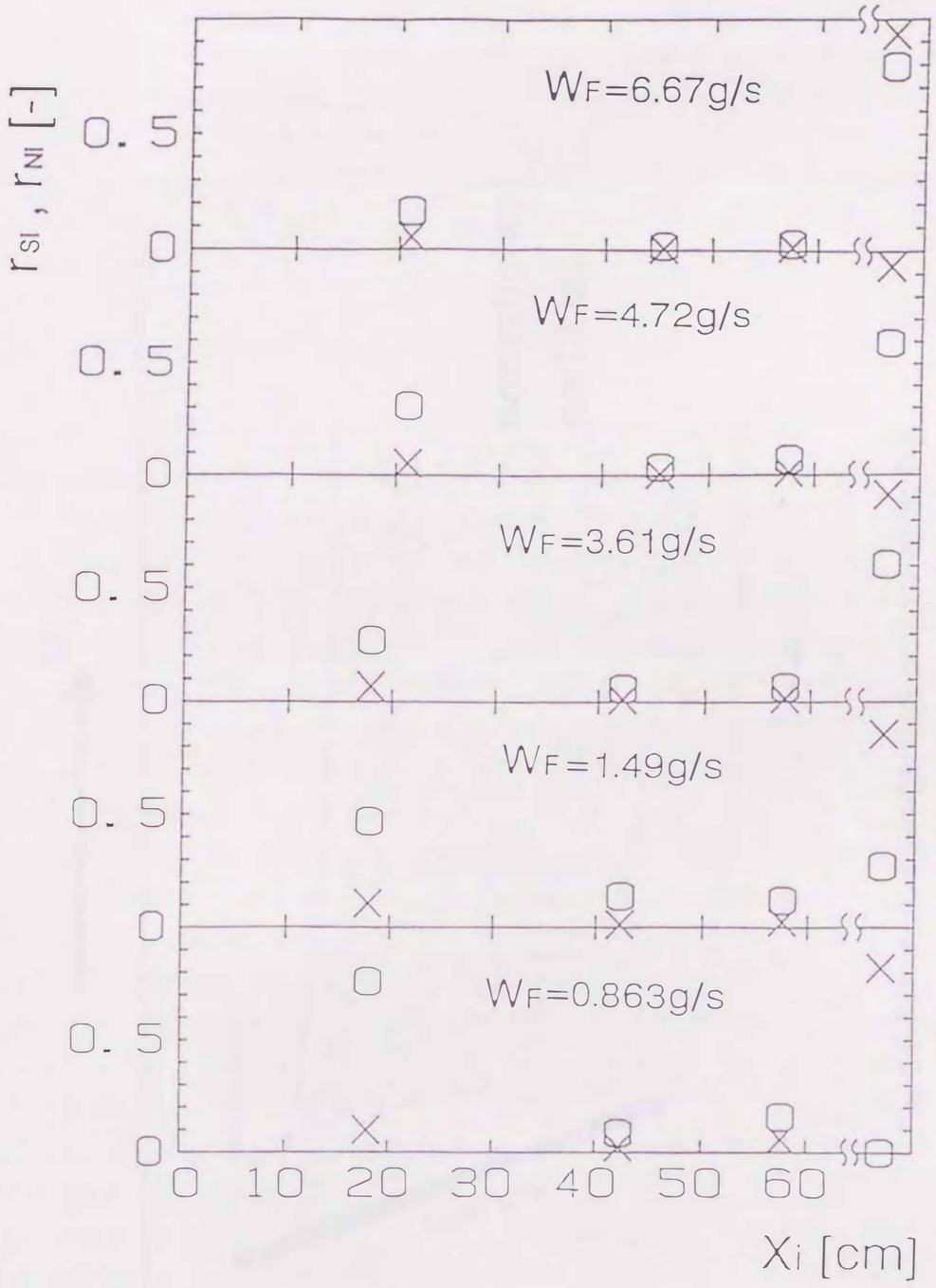


Fig.5.5 Effect of positions of recovered vessels on spherical and nonspherical particles recovery in the vessel

o sphere x nonsphere feed line : 30 cm

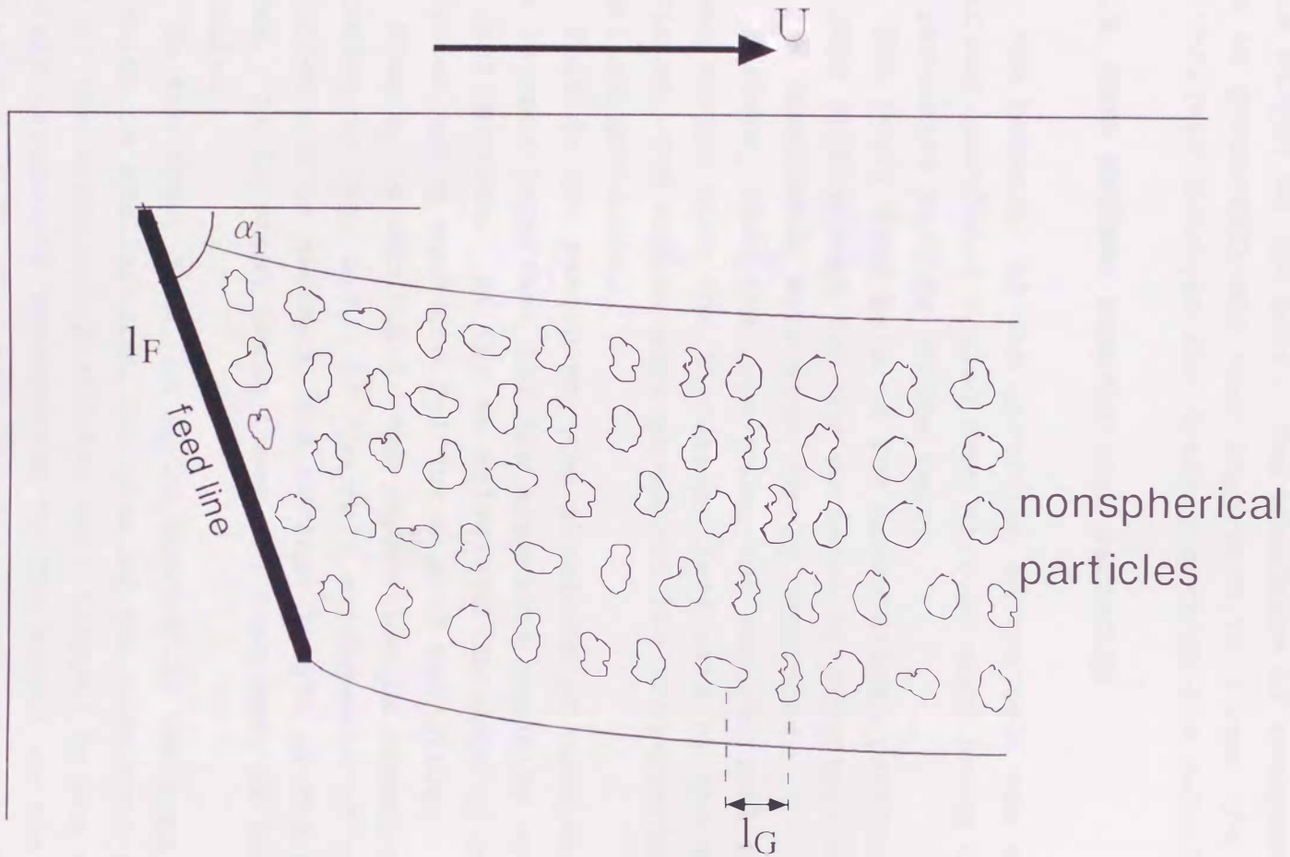


Fig. 5.6 Retention of nonspherical particles on the belt

trough.

This figure shows that the recovery distribution of spherical particles is a similar curve when the abundance of nonspherical particles is kept the same because the movement of spherical particles is interrupted by nonspherical particles, which stayed on the belt. The abundance of nonspherical particles is quantitatively very important to decide the capacity of the inclined conveyor for feeding particulate materials.

### 5.3.3 GAPS BETWEEN NONSPHERICAL PARTICLES

The behavior of the particles on the belt was as follows: Spherical particles rolled down through gaps among the nonspherical particles sitting on the belt.

The small feed rate of the nonspherical particles could keep the gaps wide enough for the movement of spherical particles. The two components were then fairly separated.

However, when the gaps among the nonspherical particles became narrow with the increasing feed rate of the nonspherical particles, the narrow gaps prevented the trajectories of the spherical particles.

This is the reason why the abundance of nonspherical particles is very important for the apparatus capacity as described in the last section. We try to calculate the gaps of nonspherical particles using equation 5-1 for a good operation.

When $\phi_N$ is about 0.3, the separation is almost perfect according to Fig. 5.7. If the rule arrangement of nonspherical particles can be assumed, the average length of the gaps, $l_G$, is 0.99mm. It is about three times the mean size of the spherical particles.

On the other hand, as $\phi_N$ is about 0.2, the gaps become 0.25 mm, which is smaller than the size of the spherical particles. Some of the spherical particles were trapped by the nonspherical particle stream and transported to the vessel on the right hand side in Fig. 5.7. The same gap size compared with the spherical particle diameter must be a minimum necessity for the perfect separation performance of the two components.

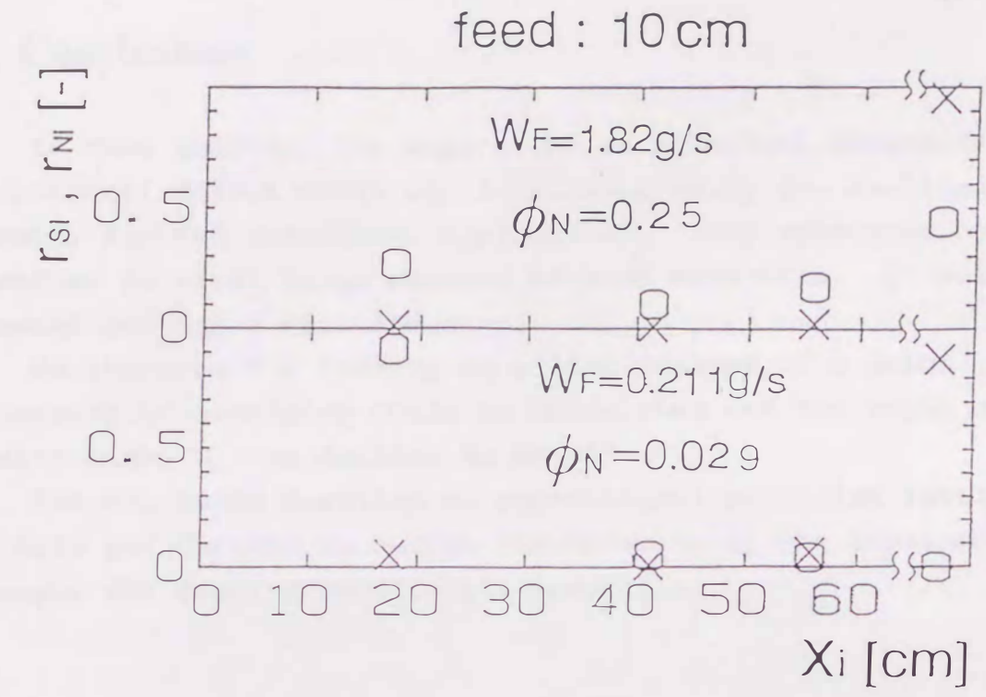


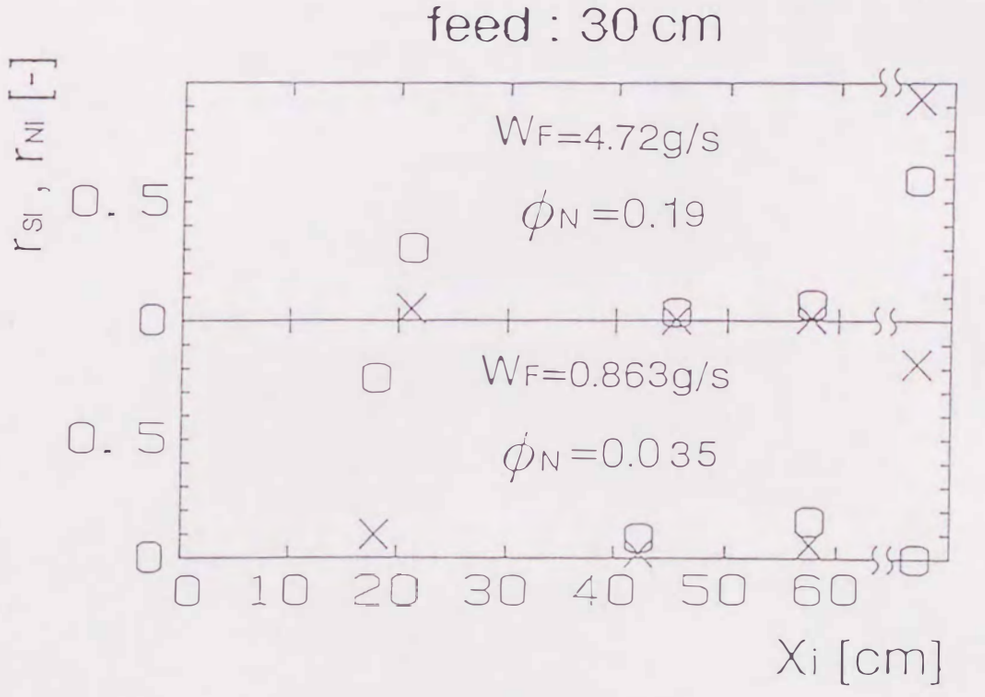


Fig.5.7 Effect of abundance fraction of nonspherical particles on spherical and nonspherical particles recovery
o sphere x nonsphere

## 5.4 Conclusions

In this chapter, the separation of spherical Cerabeads and nonspherical silica sands was introduced using the inclined conveyor for the industrial application. This apparatus has the character to treat large amounts of feed materials. It must be an excellent for a real industry.

We improved the feeding as a line instead of a point. The trajectory of particles could be calculated and the angle of the feeding line, $\alpha$, was decided to be 24°.

The abundance fraction of nonspherical particles retained on the belt was defined to decide the capacity of the inclined conveyor for feeding particulate materials.

# Chapter 6. APPLICATION OF RECYCLING USING PARTICLE SHAPE SEPARATION

## 6.1 Introduction

The recycling technique must become very important to use the limited resources of the Earth for a sustainable development as described in Chapter 1.

A suitable separation technique including the particle shape separation[5, 59-64] was applied for the various kinds of waste[5, 64-65]. However, it is sometimes difficult to crush and separate the waste, especially to pulverize a composite waste and liberate individual materials[66-68].

In this chapter, a size reducing technique for printed wiring boards is introduced, and a particle shape separation for the size-reduced mixture is discussed to recover valuable materials as good recycling samples.

This was a cooperative work with the Environmental Protection Labaratory, Dowa Mining Co., Ltd.

## 6.2 Pretreatment of scrapped electronic appliance

### 6.2.1 EXPERIMENTAL APPARATUS AND MATERIALS

The amount of printed wiring board (PWB) scrap has rapidly increased during this decade, and its industrial waste has to be treated in the near future. A recycling technology has to produce well-refined products from the PWB wastes, even though these materials are very complex in their composition.

Figure 6.1 is the cross-sectional view of PWB. Copper foil is pasted on a plastic plate reinforced by glass fiber, whose width is about 20μm. The border between them is very rugged to obtain a strong attachment. The size of the board is several 10 cm long, 3 to 5cm wide and 1.5 to 2.0mm thick. The characteristics of these components are in Table 6.1.

The experimental procedure to recover copper from PWB is shown in Fig. 6.2[69-70]. First of all, PWB was crushed to less than 10 mm by a cutter mill. After that, it was pulverized to less than 0.8 mm by the hammer mill (Seishin Co., Ltd.). The size-reduced PWB was classified by a cyclone to remove fine particles.

An inclined conveyor was used as shown in Fig. 4.1, which has 20 cm wide x 100 cm long belt for particle shape separation. Most of the copper was recovered and concentrated in the region of spherical particles.

### 6.2.2 PRETREATMENT OF PRINTED WIRING BOARD BEFORE SEPARATION

The hammer speed in the mill was fixed at 52 m/s and 78 m/s. Table 6.2 shows the mass and grade of the copper in a size-reduced PWB.

The size of the ground products became smaller at the higher hammer speed. Most of the copper particles were collected in the size range of 150 μm to 500 μm when the hammer speed was 52 m/s. A small percentage of the copper was selected for the finer part from the pneumatic cyclone at that time. However, the percentage was greater and we had to waste more valuable materials at 78

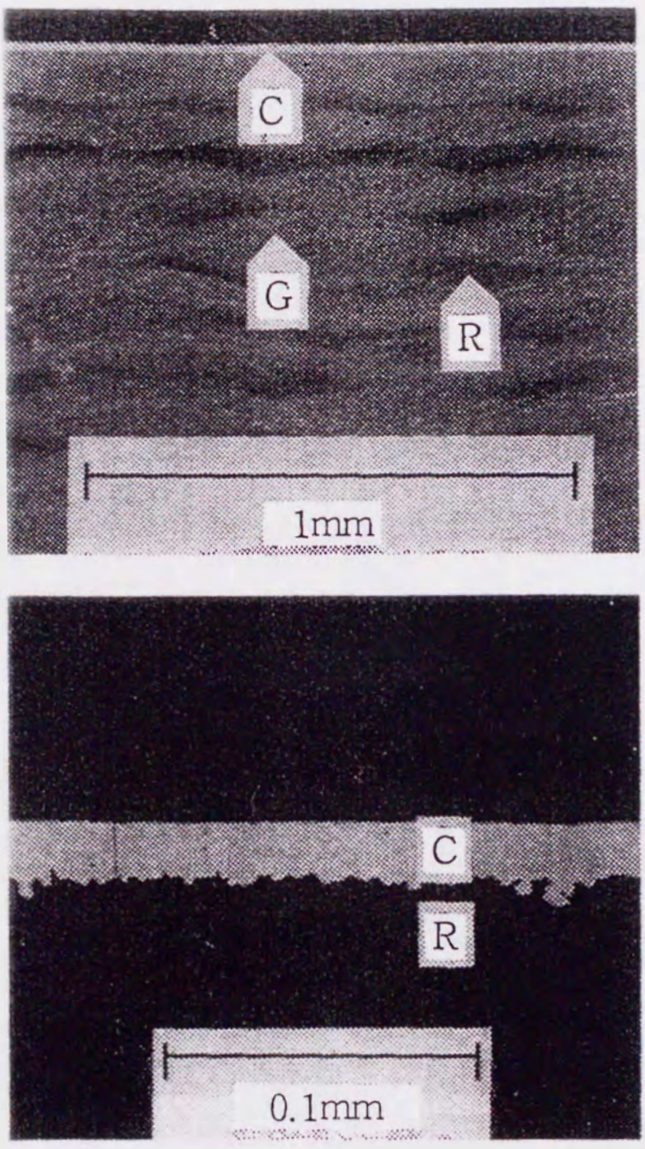


Fig.6.1 Cross–sectional view of a printed wiring board
C : copper , R : epoxy resin , G : glass

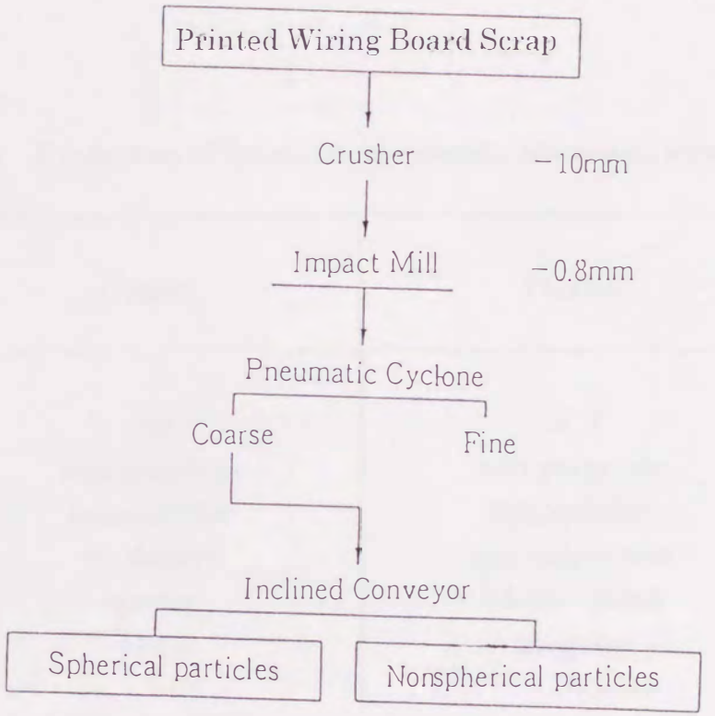


Fig.6.2 Experimental procedure

Table 6.1 Properties of the main components of printed wiring board

| Properties | Copper | Plastic | Glass |
|---|---|---|---|
| Density [g/cm³] | 8.9 | c.a. 1 | 2.5 |
| Magnetic properties | non-magnetic | non-magnetic | non-mag. |
| Surface properties | hydrophobic | hydrophobic | hydrophilic |
| Electric properties | conductive | non-conductive | non-conductive |
| Color | copper | white~green | white or transparent |
| Ground particle shape (generally) | plate | irregular | fibrous |

Table 6.2 Effect of hammer speed on the grinding product of printed wiring board

| Hammer speed | 52 m/s | | | 78 m/s | | |
|---|---|---|---|---|---|---|
| Particle size [μm] | Mass [%] | Grade [% Cu] | Cu recovery [%] | Mass [%] | Grade [% Cu] | Cu recovery [%] |
| 500～800 | 3.5 | 34.1 | 4.7 | 1.5 | 18.9 | 1.0 |
| 250～500 | 23.3 | 35.1 | 32.3 | 8.5 | 33.2 | 9.8 |
| 150～250 | 23.1 | 36.2 | 33.1 | 16.6 | 33.1 | 19.1 |
| 75～150 | 14.9 | 32.4 | 19.2 | 18.8 | 47.3 | 31.1 |
| －75 | 6.7 | 28.6 | 7.6 | 9.6 | 81.2 | 27.2 |
| Fines from cyclone | 28.5 | 2.8 | 3.1 | 45.0 | 7.5 | 11.8 |
| Total | 100.0 | 25.3 | 100.0 | 100.0 | 28.7 | 100.0 |

m/s[71].

The ground products were observed on the photograph by a secondary image electron microscope (ST800 JEOL). Almost all of the particles were completely liberated, except for the coarse particles.

We also succeeded in controlling the shape of the products at the same time. The particle shape of ductile metals like copper tends to become spherical during rolling on the inside wall of the mill, while the plastics were irregular and the glass was cylindrical. Fig. 6.3 shows the size-reduced products from PWB. It is obvious that copper was liberated in a spherical form compared to the other products.

Table 6.3 had the morphological information of ground PWB by the image analyzer. The size of the glass particles (diameter of the equivalent circle and maximum length) was the largest[72].

Circularity and the diameter of the equivalent circle were defined:

$$\text{diameter of equivalent circle} = 2(\text{area}/\pi)^{1/2} \qquad (6\text{-}1)$$

$$\text{circularity} = 4\pi(\text{area}/\text{perimeter})^{2} \qquad (6\text{-}2)$$

Copper was the most spherical, and glass was the least spherical on circularity. The circularity of plastics was high, but most of them were a little flat with an irregular shape.

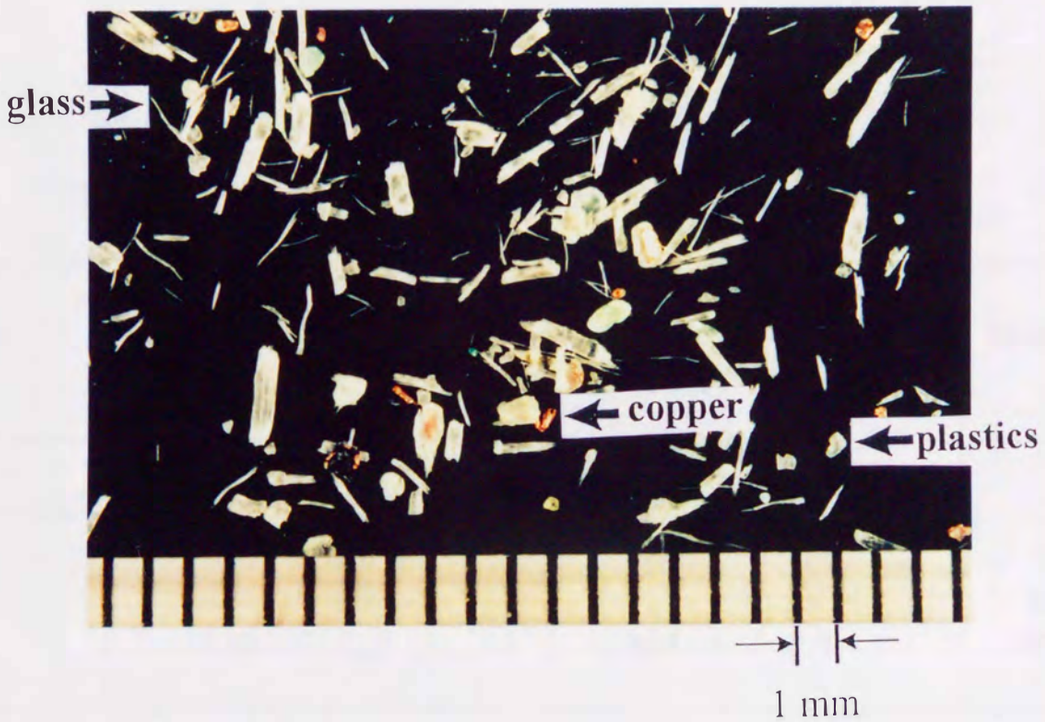


Fig.6.3 Size－reduced PWB by hammer mill

Table 6.3 Some morphological aspects of ground products

| Parameter | Circularity * | | Diameter of the equivalent circle [μm] | | Maximunm diameter [μm] | |
|---|---|---|---|---|---|---|
| Hammer speed [m/s] | 52 | 78 | 52 | 78 | 52 | 78 |
| Copper | 1.00 | 1.0 | 165 | 171 | 195 | 87 |
| Plastics | 0.86 | 0.93 | 315 | 217 | 400 | 217 |
| Glass | 0.45 | 0.30 | 424 | 200 | 876 | 568 |

* circle=1, non-circle<1

## 6.3 Recovery of copper from printed wiring board

### 6.3.1 SHAPE SEPARATION AND ANALYSIS

The same apparatus as that in Chapters 4 and 5 was used. However, the positions and scale of the collecting vessels were different as shown in Fig. 6.4. The particles of size-reduced PWB were collected in vessels 1 to 6. These particles were weighed, and the mass fraction of copper in each vessel was measured by X-ray fluorescence analysis.

When the supposed copper was a target material, the recoveries of copper and other components such as plastics and glass, in the respective vessels, were calculated by the equations in the Appendix to decide $r_{Ci}$ and $r_{Gi}$.

Generally, the recovery, $r_{CP}$, and the grade, $x_{CP}=\sum_{R} x_{Ci}W_i/\sum_{R} W_i$ of copper were useful to appreciate the separation results, especially for industrial data. Newton's separation efficiency was calculated by these values as follows:

$$\eta = r_{CP}-(1-\sum_{R}(1-x_{Ci})Wi/\sum_{P,R}(1-x_{Ci})Wi$$

$$= r_{CP}(x_{CP}-x_F)/(x_{CP}(1-x_{CF})) \qquad (6\text{-}3)$$

Belt speed varied from 18.2cm/s to 52.7cm/s. The inclined angle was set 15, 20, 25, 30, 35 or 40. The size-reduced PWB was fed at the feed point (see Fig. 6.3) on the belt with a vibration feeder, which had a V-type trough. The feed rate was small enough to neglect the interaction of the particles.

### 6.3.2 EFFECT OF BELT SPEED[73]

Belt speed and inclination angle are important operating factors. For constant inclination angle, the theoretical trajectory of the spherical particles approached that of the nonspherical ones as the belt speed increased.

Figs. 6.5 and 6.6 show the relationship between the recovery

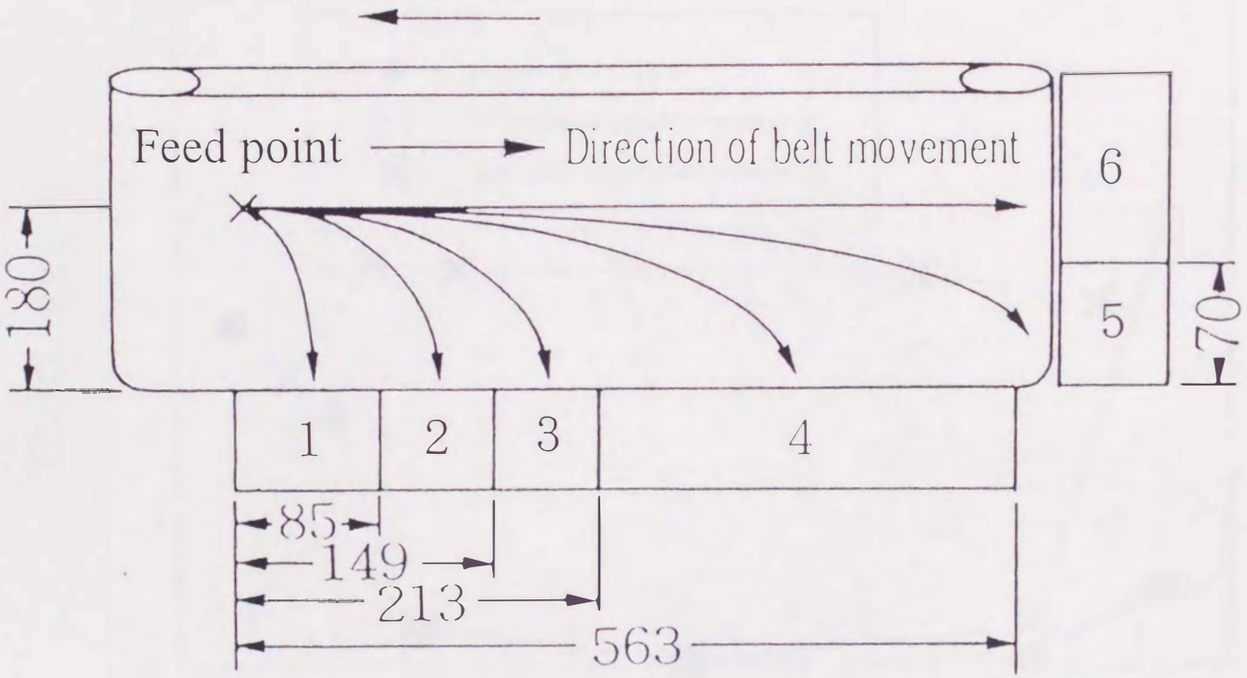


Fig.6.4 Positions of the feed point and vessels on a belt
(dimensions are in mm)

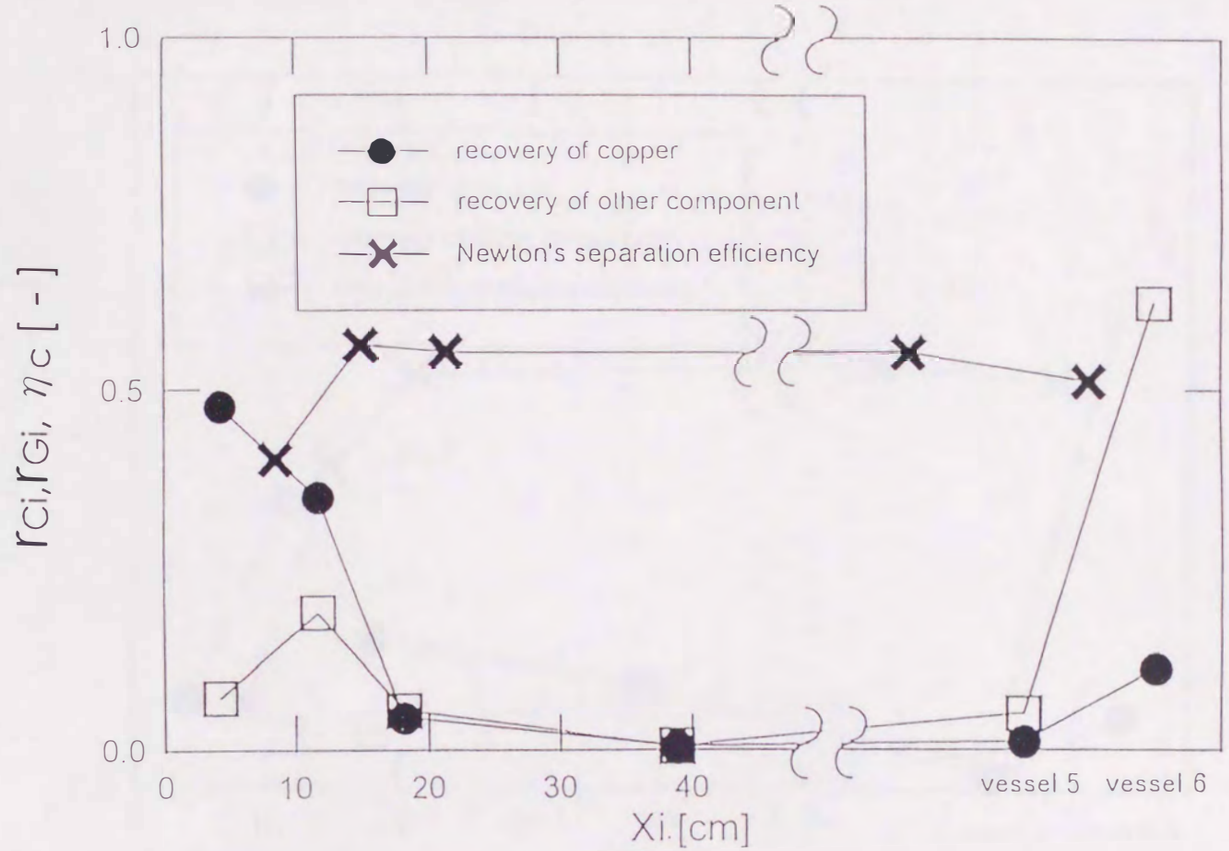


Fig.6.5 Relationship between recovery of copper, other component or Newton's separation effeciency and positions of vessels, inclined angle : 35° belt speed : 18.2 cm/s

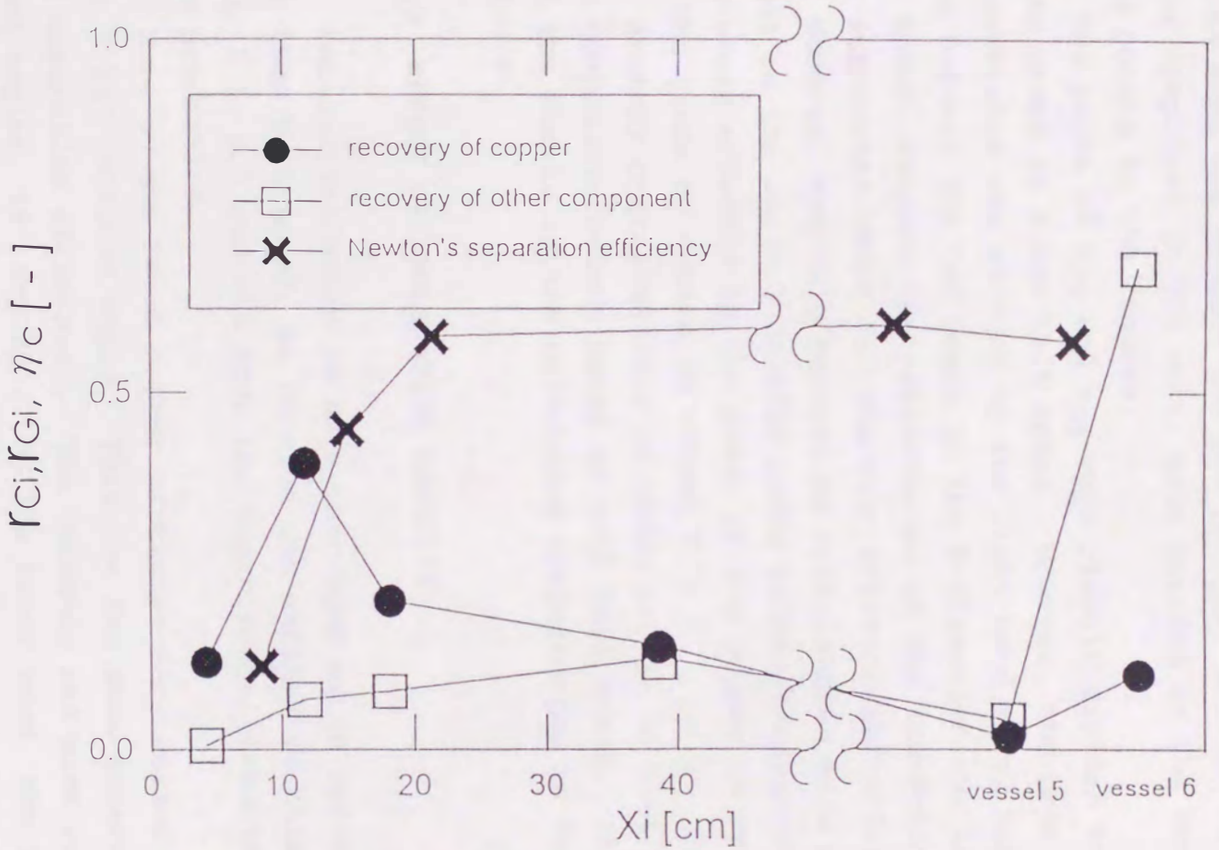


Fig.6.6 Reationship between recovery of copper, other componnent or Newton's saparation efficiency and positions of vessels, inclined angle : 35° belt speed : 52.7 cm/

of copper or the other components and the positions of the vessels for two belt speeds. Particles which did not roll down to vessels 1-4 were conveyed to the end of the belt and fell into vessels 5 and 6. The recoveries $r_{C5}, r_{C6}$ and $r_{G5}, r_{G6}$ are shown on the right hand side of these figures as reference data.

Newton's separation efficiency are also shown in these figures when the product and the residue, defined for richer and poorer component in the part, were divided by the respective cross points in the figures.

The peaks of $r_{Ci}$ and $r_{Gi}$ were clearly divided to both sides in the graph at a low belt speed. However, the peak for spherical particles was shifted to the right hand side, and the distance between the two peaks in the X-direction was less at high belt speed, because the trajectories of the low-friction particles approached those for the high-friction particles.

However, Newton's separation efficiencies were not so different on the central divided cross points because these were absolutely affected by the grade of the copper in vessels 1 to 2 and the grade of others in vessel 6.

Another characteristic of these graphs is that the peaks of both components became broad at high belt speed. This agreed with the result by the calculated trajectories in the theoretical analysis.

### 6.3.3 EFFECT OF INCLINATION ANGLE[73]

Inclination angle is more important as an operating condition than belt speed, as pointed out earlier in this paper. Figs. 6.5, 6.7 and 6.8 show the experimental results confirming this prediction.

Some of the round copper particles were collected in vessel 6 at a 25° inclined angle. This was the main reason to keep a low separation efficiency. The tendency was more remarkable at lower angles, 15° and 20°. On the other hand, the recovery distribution of copper overlapped that of the other components at 35° inclination, especially in vessels 1 and 2. However, the peaks of copper and the other components were relatively separated at 30°.

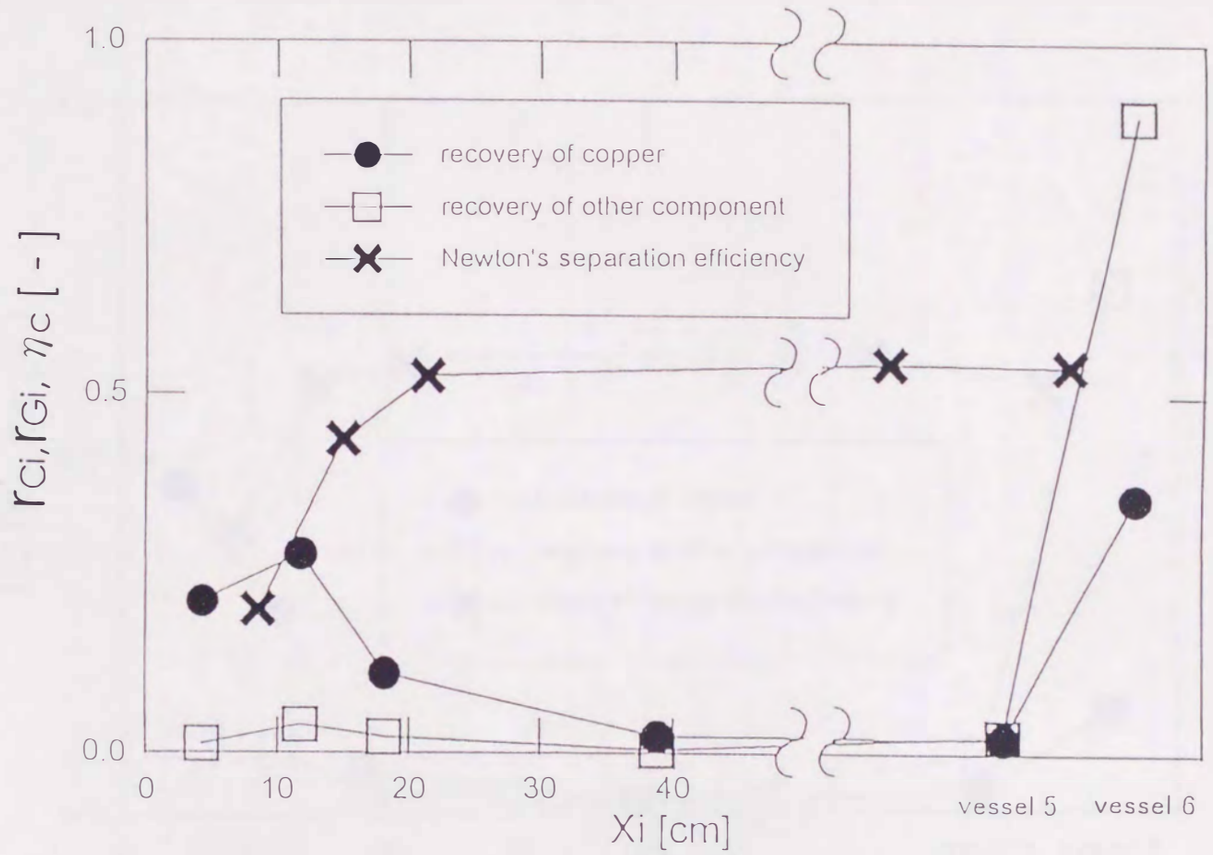


Fig.6.7 Reationship between recovery of copper, other componnent or Newton's separation efficiency and positions of vessels, inclined angle : 25° belt speed : 18.2 cm/s

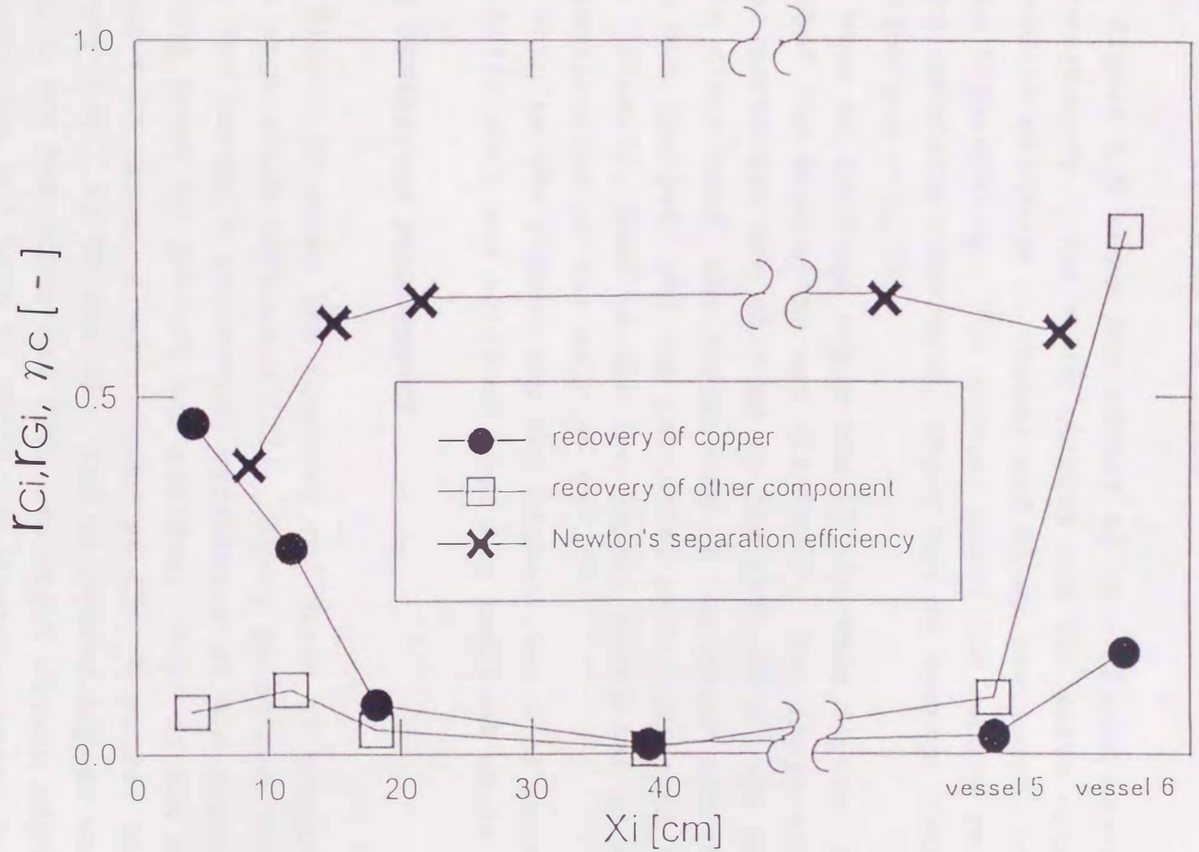


Fig.6.8 Reationship between recovery of copper, other componnent or Newton's saparation efficiency and positions of vessels, inclined angle : 30° belt speed : 18.2 cm/s

It was clear for Newton's separation efficiencies. The highest one was 0.643 when the inclined angle was 30° and the dividing point of the product and the residue was between vessels 4 and 5.

### 6.3.4 TRAJECTORIES OF PARTICLES

Figure 6.9 shows the effect of an inclined angle on a particle trajectory. The black circles and the white squares indicate the median distance of copper and other particles, respectively, to the X-direction. The segment meant the median range for 40% of the particles recovered, which had an average character of friction and roll[73].

When an inclined angle was 15° in this figure, it was obvious that the separation was difficult. The trajectory of the copper particles was shifted to the left hand side on the belt. On the other hand, the trajectory of the other component was still not changed, and the particles were collected in vessels 5 to 6. Finally, some of the non-copper particles were rolled by the inclination of the belt at 35°.

This is the reason why the highest value of Newton's separation efficiency was obtained when the inclined angle was 30°.

### 6.3.5 SEPARATION PERFORMANCE

Fig. 6.10 shows the recovery and grade of copper and Newton's separation efficiency[72]. Every point has the highest value for Newton's separation efficiency at the appropriate dividing point of product and residue. Most of the collected particles in vessel 1 were copper at 15°; however, the recovery was very low. At 30 and 35°, the recovered copper was 50% in vessel 1 and the grade was 80%. We might obtain higher recovery for recycling and have to shift the dividing point to the right hand side on the belt.

The recovery and grade of copper are presented in Fig. 6.11. Most of the collected particles in vessel 1 were copper at 15°; however, the recovery was very low. At 30° and 35°, the recovered copper was 50% in vessel 1, and the grade was 80%. We might

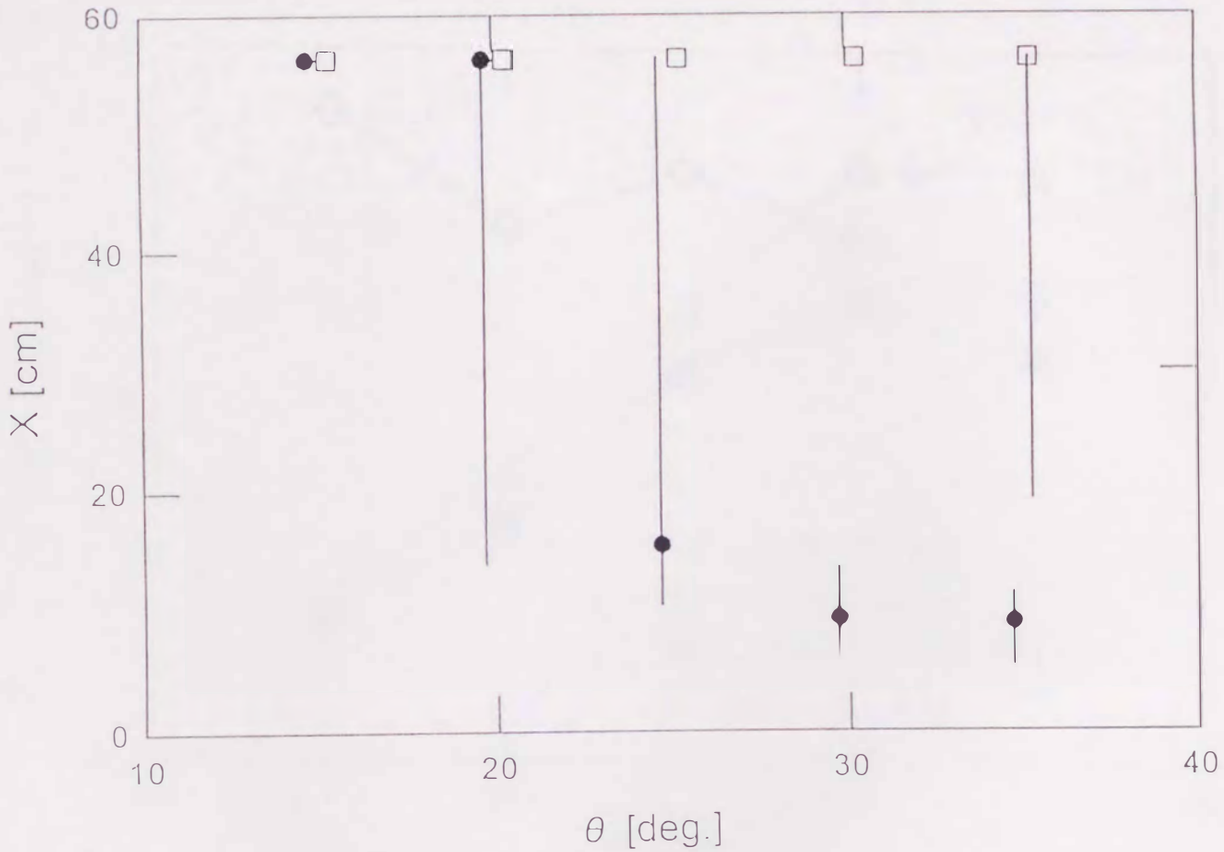


Fig.6.9 Reationship between recovery of particles and inclined angle : ● , copper ; □, other component ; belt speed : 18.2 cm/s

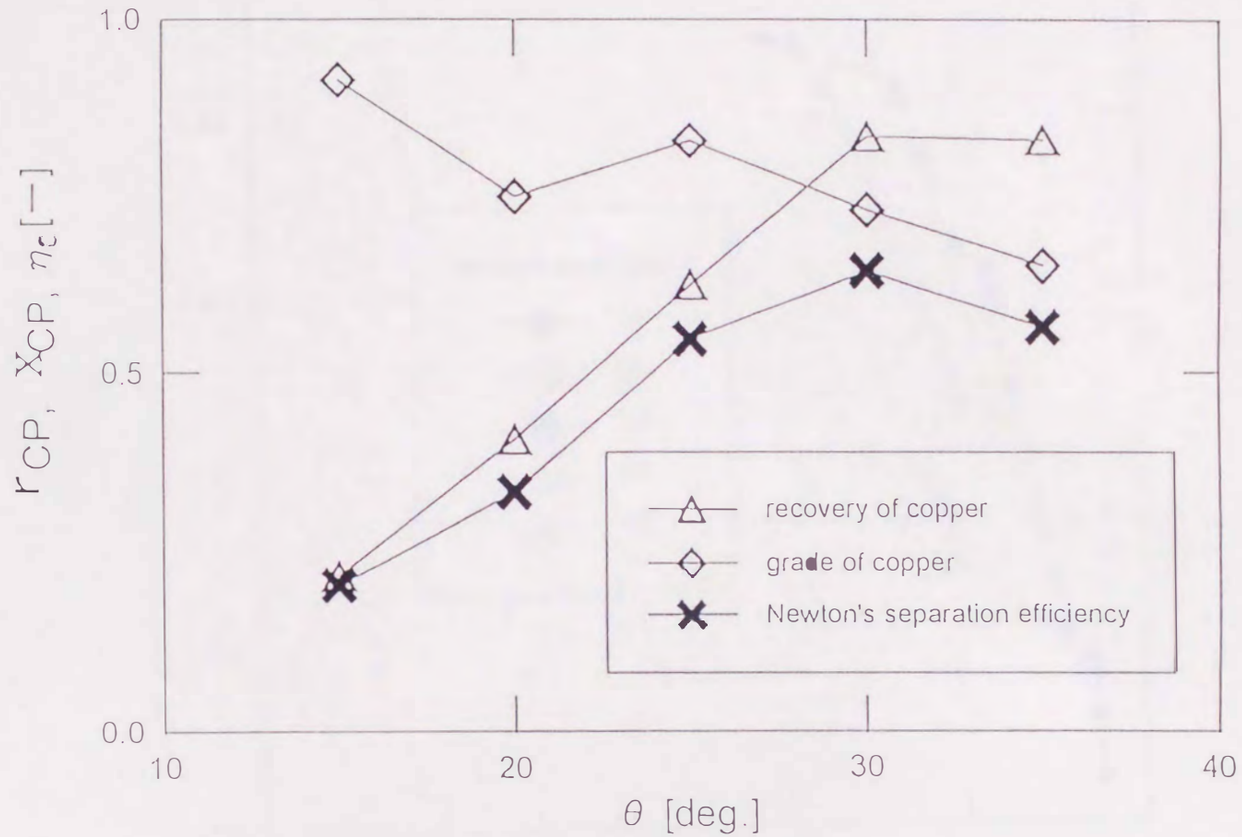


Fig.6.10 Recovery of copper, grade of copper, Newton's separation efficiency
belt speed : 18.2 cm/s

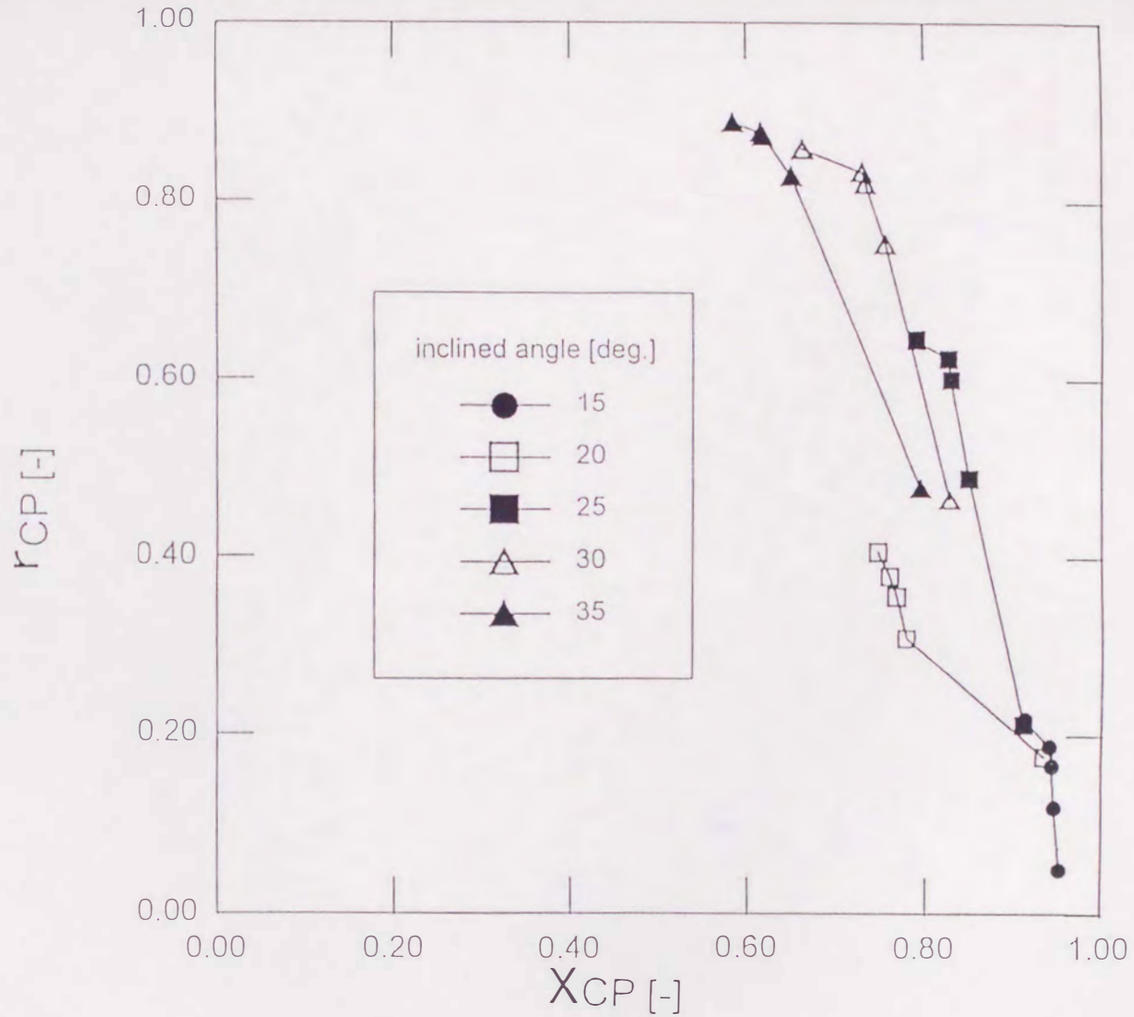


Fig.6.11 Relationship between recovery and grade of copper
belt speed : 18.2 cm/s

obtain higher recovery for recycling and have to shift the cut point of the product to the right hand side.

The 83.3% recovery and 72.9% grade were achieved at the same time when an inclined angle was 30° and the belt speed was 18.2 m/s.

## 6.4 Conclusions

This chapter discusses the recovery of copper from the printed wiring board scrap for resource recycling. In the size-reduction step, the hammer mill was used for not only the liberation of copper but also controlling the shape of ground product.

The spherical copper particles could be separated from the irregular plastics and needle-like glass fiber. The inclined conveyor was very suitable for the treatment of large amounts of materials like this resource recycling.

More than 80% recovery and 70% grade of copper was obtained in the experimental result.

# Chapter 7. SUMMARY AND CONCLUSIONS

This thesis concerns the development and separation performance of particle shape separators. Three types of separators were developed as rolling and sliding types. Each of them has its own characteristics.

An inclined vibration plate has the possibility of accurate separation or sorting by shape. A mixture of glass beads and silica sands were sorted, and the separation characteristics based on particle shape were examined using a mixture containing particles with very different shapes. It was found that Newton's separation efficiency attained 0.99. The recoveries of spherical and nonspherical particles were almost 1.

An accurate apparatus like an inclined vibration plate must be used by not only a shape separator but also a particle shape analyzer. It has the possibility to treat valuable materials like jewels on particle shape separation, too.

A new apparatus for particle shape distinction driven by horizontally circulated vibration has been devised, and successful separation results not only between spheres and nonspheres but also among nonspherical particles have been demonstrated.

This apparatus has a unique movement of particles on the plate. The basic kinetic studies for particles on the horizontally vibrating plate were investigated based on the research with gyro shifter sieving. However, the movement of particles beside a circlar wall was really characteristic and calculated using our model.

Most of the experimental results for 500 to 850 μm particles could be explained by the theoretical trajectories. We think our theory can be applied to particles larger than 200 μm, but adhesion and agglomeration become very serious problems for separation of fine particles and powders.

It is possible that this apparatus is applicable for the separation of finer particles. The shape separation of about 100 μm glass beads and powders has been successful; however, the separation efficiency was not so high. We believe that finer particles could be treated and better separation efficiency would be obtained for the improvement of the apparatus as if the forces

working on the particles were stronger and the adhesion became smaller.

An inclined conveyor was developed as a new type of particle shape separator for the purpose of processing large amounts of feed materials and a simple structure. They are most important characteristics of this apparatus for an industrial application.

The movement of particles on the belt was analyzed by kinetic formula. A difference in the trajectories between spherical and nonspherical particles is necessary for an efficient separation. Therefore, the tangent of the angle must be intermediate between the two particle friction coefficients.

The conveyor was experimentally investigated, and it became clear that the inclination angle is the most important operating condition compared to other factors. It corresponded to the results of the theoretical analysis.

Two kinds of application were described in this thesis. The first one is a recovery of artificial ceramic beads from reclaimed foundry sands. A larger amount of particulate materials could be processed because of the improvement in the feeding as a line instead of a point. More than ten times of the materials could be treated with 30 cm line feeding compared with a point feeding.

The abundance fraction of nonspherical particles was very important in deciding the upper limit of a processed amount. It was related to avoiding interactions of spherical and nonspherical particles.

The second application was a very interesting example applied to resource recycling. The waste printed wiring boards mainly consist of copper, plastics and glass fiber. It was size reduced to liberate copper from other materials. The copper particles became spherical, and the other materials were nonspherical at the same time.

The inclined conveyor was applied to separate spherical copper particles from the other materials. Copper could be recovered from waste printed wiring board as a high recovery and grade. We can offer a new dry process to treat waste electric products.

We have to search for more applications, especially on an

industrial scale in order to maintain our global environment and develop new functional materials. Separation is a key technology for all kinds of waste treatment. Shape separation is a new field for an industrial scale. It must be focused on resource recycling in the near future.

# APPENDIX

When the feed can be divided into two components as product and residue after a separation, recoveries of spherical and nonspherical particles in the respective vessels were defined by the following equations:

$$r_{Si} = x_i W_i \,/\, x_F W_F \tag{A-1}$$

$$r_{Ni} = (1 - x_i) W_i \,/\, (1 - x_F) W_F \tag{A-2}$$

where $x_i$ and $W_i$ are, respectively, the fraction of spherical particles and the weight of the collected particles in the position of vessel i, whose position coordinate is $X_i$ in the y-direction on the inclined vibration plate or the x-direction on the inclined conveyor from the feed point to the center of the vessel i. $W_F$ is the weight of the feed. $(1-x_i)$ and $(1-x_F)$ are the fractions of nonspherical particles in vessel i and the feed, respectively.

Newton's separation efficiency, $\eta$, and recoveries of spherical and nonspherical particles, $r_S$, $r_N$, were defined:

$$\eta = r_{SP} - (1 - r_{NP}) \tag{A-3}$$

$$r_{SP} = \sum_{P} x_{Si} W_i \,/\, x_{SF} W_F \tag{A-4}$$

$$r_{NR} = \sum_{R} (1 - x_{Si}) W_i \,/\, (1 - x_{SF}) W_F \tag{A-5}$$

We can decide the appropriate dividing point for the maximum value of Newton's separation efficiency in Chapter 2, 3, 5 and 6. $\eta_{max}$ is defined by the biggest value of $\eta$ at that time. $\eta_{max}$ was decided under an individual experimental condition.

In Chapter 6, the copper was a target material. The recoveries of copper and other components, such as plastics and glass, $r_{Ci}$ and $r_{Gi}$, in the respective vessels were used instead of $r_{Si}$ and $r_{Ni}$.

$$r_{Ci} = x_{Ci}W_i \,/\, x_{CF}W_F \qquad \text{(A-6)}$$

$$r_{Gi} = (1 - x_{Ci})W_i \,/\, (1 - x_{CF})W_F \qquad \text{(A-7)}$$

Where the mass fraction of copper, $x_{Ci}$, was used instead of $x_i$.

For the same reason, we defined the following factors:

$$\eta_C = r_{CP} - (1 - r_{GP}) \qquad \text{(A-8)}$$

$$r_{CP} = \sum_P x_{Ci}W_i \,/\, x_{CF}W_F \qquad \text{(A-9)}$$

$$r_{GR} = \sum_R (1 - x_{Ci})W_i \,/\, x_{CF}W_F \qquad \text{(A-10)}$$

# NOMENCLATURE

$a$ : amplitude of vibration [m]

$\mathbf{a}$ : acceleration vector of particles [$m/s^2$]

$d_N$ : mean diameter of nonspherical particles [m]

$D_v$ : diameter of circular wall on horizontally circular motion [m]

$f$ : frequency of vibration [1/s]

$\mathbf{F}$ : partial force vector of gravity in the slope direction [N]

$F$ : Y-component of $\mathbf{F}$ [N]

$F_S/F_N$ : feed ratio of spherical and nonspherical particles [-]

$F_a$ : $=\mu mg$ [kg $m/s^2$]

$g$ : gravity acceleration [$m/s^2$]

$\mathbf{g}$ : gravity acceleration vector [$m/s^2$]

$K$ : vibration intensity [-]

$l_F$ : length of feed line [m]

$l_G$ : average gap length of nonspherical particles on inclined conveyor [m]

$m$ : mass of a particle [kg]

$N$ : normal reaction [N]

$P$ : $=m\omega^2 R$ [kg $m/s^2$]

$P_a$ : $=m\omega^2 r_a$ [kg $m/s^2$]

$P_r$ : $=m\omega^2 r_r$ [kg $m/s^2$]

$r_a$ : radius of Scott circle [m]

$r_{Ni}$ : recovery of nonspherical particles in vessel i [-]

$r_{NR}$ : recovery of nonspherical particles in residue [-]

$r_{Si}$ : recovery of spherical particles in vessel i [-]

$r_{SP}$ : recovery of spherical particles in product [-]

$r_{CP}$ : recovery of copper in product [-]

$r_{Ci}$ : recovery of copper in vessel i [-]

$r_{Gi}$ : recovery of plastics and glass in vessel i [-]

$r_{GR}$ : recovery of plastics and glass in residue [-]

$r_r$ : radius of Zukowski circle [m]

$\mathbf{R}$ : friction force vector [N]

$R$ : radius of circular motion [m]

$R_x$ : x component of friction force [N]
$R_y$ : y component of friction force [N]
$t$ : time [s]
$u$ : velocity of particle [m/s]
$u_{av}$ : average transport velocity of silica sands in inclined vibration plate [m/s]
$\mathbf{u}$ : velocity vector of particle [m/s]
$\mathbf{u}_p$ : velocity vector of particle in the absolute movement [m]
$\mathbf{u}_t$ : velocity vector of particle for circular motion plate [m]
$U$ : belt transportation velocity [m/s]
$\mathbf{v}$ : relative velocity vector of particles with respect to the inclined conveyor [m/s]
$\mathbf{V}$ : velocity vector of particles [m/s]
$V_{ox}$ : initial velocity of partilces [m/s]
$V_x$ : X-component of particles velocity [m/s]
$V_y$ : Y-component of particles velocity [m/s]
$W_F$ : mass of feed per unit time [kg/s]
$W_i$ : mass of particles recovered in a vessel i per unit time [kg/s]
$W_P$ : mass of products per unit time [kg/s]
$W_R$ : mass of residues per unit time [kg/s]
$x_{CF}$ : mass fraction of copper in feed [-]
$x_{Ci}$ : mass fraction of copper in vessel i [-]
$x_{CP}$ : mass fraction of copper in product [-]
$x_F$ : mass fraction of spherical particles in feed [-]
$x_i$ : mass fraction of spherical particles in a vessel i [-]
$x_P$ : mass fraction of spherical particles in products [-]
$x_R$ : mass fraction of spherical particles in residues [-]
$X_i$ : displacement of vessel i in the X-direction from the feed point [m]
$X$ : rectangular coordinate [m]
$X_p$ : rectangular coordinate in the absolute movement [m]
$X_t$ : rectangular coordinate for circular motion plate [m]
$Y$ : rectangular coordinate [m]
$Y_p$ : rectangular coordinate in the absolute movement [m]

$Y_t$ : rectangular coordinate for circular motion plate [m]

$Z$ : rectangular coordinate [m]

$Z_p$ : rectangular coordinate in the absolute movement [m]

$Z_t$ : rectangular coordinate for circular motion plate [m]

$\alpha$ : angle of throw in inclined vibration plate [-]

$\alpha_1$ : angle between the feed line and direction of belt movement [-]

$\beta$ : angular displacement [-]

$\varepsilon_N$ : degree of sufficiency space of nonspherical particle [-]

$\phi_N$ : abundance fraction of nonspherical particles on the belt [-]

$\eta$ : Newton's separation efficiency [-]

$\eta_c$ : Newton's separation efficiency of copper [-]

$\eta_{max}$ : maximum Newton's separation efficiency [-]

$\mu$ : friction force coefficient [-]

$\theta$ : inclined angle of inclined vibration plate and inclined conveyor [deg.]

$\rho_N$ : density of nonspherical particles [$kg/m^3$]

$\omega$ : angular velocity [1/s]

$\psi$ : shape factor [-]

# ACKNOWLEDGMENTS

This thesis is the result of a research project funded by the Ministry of International Trade and Industry. Many people have contributed to this project. Without their support, this thesis would not have been possible.

I am really indebted to Professor Sukeyuki Mori, Department of Mining Engineering, Faculty of Engineering, Kyusyu University, for his scholastic guidance in completing this thesis. I would also like to thank Professor Eiji Izawa, Department of Mining Engineering, Faculty of Engineering, Kyusyu University, Professor Shigeharu Morooka, Department of Chemical Science and Technology, Faculty of Engineering, Kyusyu University and Professor Atsuo Sueoka, Department of Energy and Mechanical Engineering, Faculty of Engineering, Kyusyu University for their invaluable advice.

I thank Mr. Takeshi Hara, Mr. Takashi Furuyama and Mr. Atsushi Shibayama, Department of Mining Engineering, Faculty of Engineering, Kyusyu University, for their helpful comments and suggestions.

I am very grateful to Dr. Hiroyuki Iwata, Senior Researcher of the Material Processing Department, National Institute for Resources and Environment (NIRE), for giving me the opportunity to perform this research and for his stimulating support and discussions. I am also grateful to Dr. Shigehisa Endoh, Chief of the Material Handling and Characterization Division, Material Processing Department, NIRE, for his daily guidance, through tough discussions, useful comments and many various suggestions. I would also like to thank Mr. Mitsuru Yamamoto, previous Senior Researcher of the Material Handling and Characterization Division, Material Processing Department, NIRE, for his kind and helpful technical support.

I am very thankful to Dr. Hiroshi Sakamoto, Chief Senior Researcher of NIRE and Dr. Atsumu Tsunashima, Director of the Material Processing Department, NIRE, for their continuous and helpful support, also to Professor Brian Scarllet, Department of Chemical and Material Science, Delft University of Technology, for his helpful discussions.

I am indebted to Dr. Chihiro Izumikawa, Director of Environ-

mental Protection Laboratory, Dowa Mining Co., Ltd., Mr. Tadashi Honma, President of Japan Eriz Magnetics Co., Ltd., and Mr. Yoshiaki Hamano, Kawatetsu Mining Co., Ltd., for their cooperative research work. I would also like to thank Mr. Shigeki Koyanaka, Material Handling and Characterization Division, Material Processing Department, NIRE, for his strong support, Mr. Takahiro Hayashi, Mr. Kaoru Masuda and Mr. Shigeyuki Suzuki, Material Handling and Characterization Division, Material Processing Department, NIRE, for their technical help, all my colleagues at the Materials Processing Department, for their comments and suggestions during this research.

Finally, I would like to thank my brother, Mr. Kozo Ohya, for his helpful support and encouragement.

# REFERENCES


[1]Kennedy,P.: 21seiki no Nanmonnisonaete, (1993) Soshisya(Tokyo)

[2]Meadows,D.N., Meadows, D.L., Randers,J.: Genkai wo Koete, (1992) Daiyamondosya(Tokyo)

[3]Nishiyama, T.: Shigenkeizaigaku no Susume, (1993) Chuoukoron-sya(Tokyo)

[4]Wills,B.A.: Mineral Processing Technology, (1992) Pergamon Press(Oxford)

[5]Harada,T.: Shigen Recycling, (1991) Nikkankogyoshinbunsha(Tokyo)

[6]Nanjo,M.: Senkoseireniho in Tohoku University, 43, 248 (1987)

[7]Goto,K.: Funryutaikogaku, 107 (1985) Makisyoten(Tokyo)

[8]Yamamoto,H., Ikazaki,F., Endoh,S., Tsubaki,J.: Ryusikei Kei-sokugijutsu, 215 (1994) Nikkankogyoshinbunsya(Tokyo)

[9]Endoh,S.: J. Soc. Pow. Tech. Japan, 24, 40 (1987)

[10]Moro,T., Iwata,H., Ohya,H.: Reports of National Research Institute for Pollution and Resources (1989)

[11]Ohya,H.: Funtai to Kogyo, 23, 29 (1991)

[12]Iwata,H., Ohya,H., Endoh,S.: Resource Processing, 40, 77 (1993)

[13]Beresford,D.O.: U. S. Patent 2,724,498 (1955)

[14]Glezen,W.H., Ludwick,J.C.:J. Sediment Petrology, 33, 23 (1963)

[15]Waldie,B.: Powder Tech., 7, 244 (1973)

[16]Thompson,E.: U. S. Patent 871,536 (1907)

[17]Prinz,F.: U. S. Patent 897,489(1908)

[18]Lotozky,A.: U. S. Patent 1,190,926(1916)

[19]Ulrich,C.J.: U. S. Patent 1,291,278(1919)

[20]Carpenter,F.G., Deitz,V.R.: J. Res. Nat. bureaw of Standards, 47, 139 (1951)

[21]Riley,G.S.: Powder Tech., 2, 315 (1968)

[22]Klar,E.: Powder Tech., 3, 313 (1969)

[23]Sugimoto,M., Yamamoto,K., Williams,J.C.: J. Chem. Eng. Japan, 10, 137 (1977)

[24]Yamamoto,K., Sugimoto,M.: J. Soc. Pow. Tech. Japan, 16, 521 (1979)

[25]Yamamoto,K. ,Sugimoto,M.: J. Soc. Pow. Tech. Japan, 22, 626

(1985)
[26]Yamamoto,K., Sugimoto,M.: J. Soc. Pow. Tech. Japan, 22, 813 (1985)
[27]Kago,T., Yamamoto, K., Sugimoto,M.: Proc. Soc. Pow. Tech. Japan Autum Meeting, Tokyo (1989)
[28]Furuuchi,M., Nakagawa,M., SuzukiM., Tsuyumine,H., Goto,K.: Powder Tech., 50, 137 (1987)
[29]Furuuchi,M., Goto,K.: Powder Tech., 54, 31 (1988)
[30]Abe,E., Hirosue,H.: J. Chem. Eng. Japan, 15, 323 (1982)
[31]Meloy,T.P., Clark,N., Durney,T.E., Pitchumani,B.: Chem. Eng. Sci., 40, 1077 (1985)
[32]Clark,N., Meloy,T.P.: Powder Tech., 54, 271 (1988)
[33]Endoh,S., Koga,Y., Yamaguchi,K.: Powder Sci. Tech. Japan, 2, 7 (1984)
[34]Hsyng,N.B., Beddow,J.K., Vetter,A.F.: Proc. 8th Powder and Bulk Solids Conf. (1983)
[35]Furuuchi,M., Yamada,C., Goto,K.: Proc. 2nd World Congress Particle Tech., Kyoto (1990)
[36]Sano,S., Yashima,S.: Proc. Min. Met. Inst. Japan, T-1 (1987)
[37]Sano,S., Nikaidoh,M.: Proc. 2nd World Congress Particle Tech., Kyoto (1990)
[38]Mulari,C., Pichumani, B.,Clark,N.N.: Inter. J. Min. Proc., 18, 237 (1986)
[39]Sugimoto,N., Akiyama,K., Tokoro,K., Masuda,T.: Kikai Gakkai Ronbunsyu, 27, 1494 (1961)
[40]Sakaguchi,K., Taniguchi,O.: Riken Hokoku, 47, 125 (1971)
[41]Endoh,S.: Powder Technology, 50, 103 (1987)
[42]Endoh,S., Ohya,H., Ikeda,C., Iwata,H.: Full Text of CHISA Conference, C5, 128 (1993)
[43]Miwa,S.: Furuiwakedokuhon, 126 (1969)
Sangyogijutsusenta(Tokyo)
[44]Miwa,S.: Funtinofuruiwake, 245 (1965)
Nikankogyoshinbunsha(Tokyo)
[45]Iwata,H., Ohya,H., Yamamoto,M., Masuda,K., Endoh,S.: Proc. Soc. Pow. Tech. Japan Spring Meeting, Kyoto (1991)
[46]Iwata,H., Ohya,H., Masuda,K., Endoh,S.: Full Text of CHISA Conference, C5, 145 (1993)
[47]Ohya,H., Koyanaka,S., Endoh,S., Iwata,H.: Proc. Min. Mat.

Proc. Inst. Japan Spring Meeting, Chiba (1991)
[48]Sakaguchi,K.: Kikai Gakkai Ronbunsyu, 43, 130 (1977)
[49]Taniguchi,O., Sakata,M., Suzuki,Y., Osanai,Y.: Kikai Gakkai Ronbunsyu, 28, 485 (1962)
[50]Sakaguchi,K., Taniguchi,O.: Kikai Gakkai Ronbunsyu, 38, 103 (1972)
[51]Sakaguchi,K., Taniguchi,O.: Kikai Gakkai Ronbunsyu, 35, 2183 (1969)
[52]Sugimoto,N., Akiyama,K., Tokoro,K., Masuda,T.: Kikai Gakkai Ronbunsyu, 27, 1503 (1961)
[53]Iwata,H., Ohya,H., Endoh,S., Masuda,K., Koyanaka,S., Nemeth,L.: Full Text of CHISA Conference, P7, 55 (1996)
[54]Ohya,H., Endoh,S., Yamamoto,M., Iwata,H., Ikeda,C.: Powder Technology, 77, 55 (1993)
[55]Endoh,S., Ohya,H., Iwata,H.: Proceedings of the 4th Asian Conference on Fluidized Bed and Three Phase Reactor, 1, 79 (1993)
[56]Lee,M., Oh,H., Koyanaka,S., Ohya,H., Endoh,S.: Journal of the Sociaty of Powder Technology, Japan, 34, 515 (1997)
[57]Iwata,H., Endoh,S., Ohya,H., Gyenis,J.: Proceedings of the 5th World Congress of Chmical Engineering, 6, 374 (1996)
[58]Ohya,H., Yamamoto,M., Endoh,S., Iwata,H., Honma,T., Hamano,Y.: Full Text of CHISA Conference, C5, 129 (1993)
[59]Nikkei Business Publications Inc.: Nikkei Materials and Technology, 126, 9 (1993)
[60]Iji,M., Yokoyama,S.,Nakahara,Y.: NEC giho, 46, 55 (1993)
[61]Endoh,S., Koyanaka,S.: Chemical Engineering, 11, 17 (1994)
[62]Koyanaka,S., Endoh,S., Iwata,H.: Journal of the Sociaty of Powder Technology, Japan, 32, 10 (1995)
[63]Koyanaka,S., Endoh,S., Ohya,H., Iwata,H.: Proceedings of China-Janan Symposium on Particuology, 1, 499 (1996)
[64]Koyanaka,S., Endoh,S., Ohya,H., Iwata,H.: Shigen to Kankyo, 4, 49 (1995)
[65]Endoh,S.: Zairyogijutsu, 13, 267 (1995)
[66]Austin,L.G., Jindal,V.K., gotsis,C.: Powder Technology, 42, 199 (1979)
[67]Hnilica,P., Thyn,J., Pechlak,B.: Powder Technology, 45, 183 (1986)
[68]Koyanaka,S., Endoh,S., Ohya,H., Iwata,H.: Powder Technology,

90, 135 (1997)
[69]Iwata,H, Endoh,S., Ohya,H., Izumikawa,C.: Japan Patent 275,063 (1903)
[70]Izumikawa,C., Iwata,H, Endoh,S., Ohya,H.: U. S. Patent 08/1391,344(1996)
[71]Ohya,H., Koyanaka,S., Endoh,S., Iwata,H.: Proceedings of 6th Symposium on Particle Size Analysis, Environment and Powder Technology, 1, 47 (1995)
[72]Izumikawa,C., Sasaki,H., Ohya,H., Endoh,S., Iwata,H.: Journal of the Sociaty of Powder Technology, Japan, 32, 17 (1995)
[73]Ohya,H., Koyanaka,S., Endoh,S., Iwata,H.: Resource Processing, 44, 3 (1997)

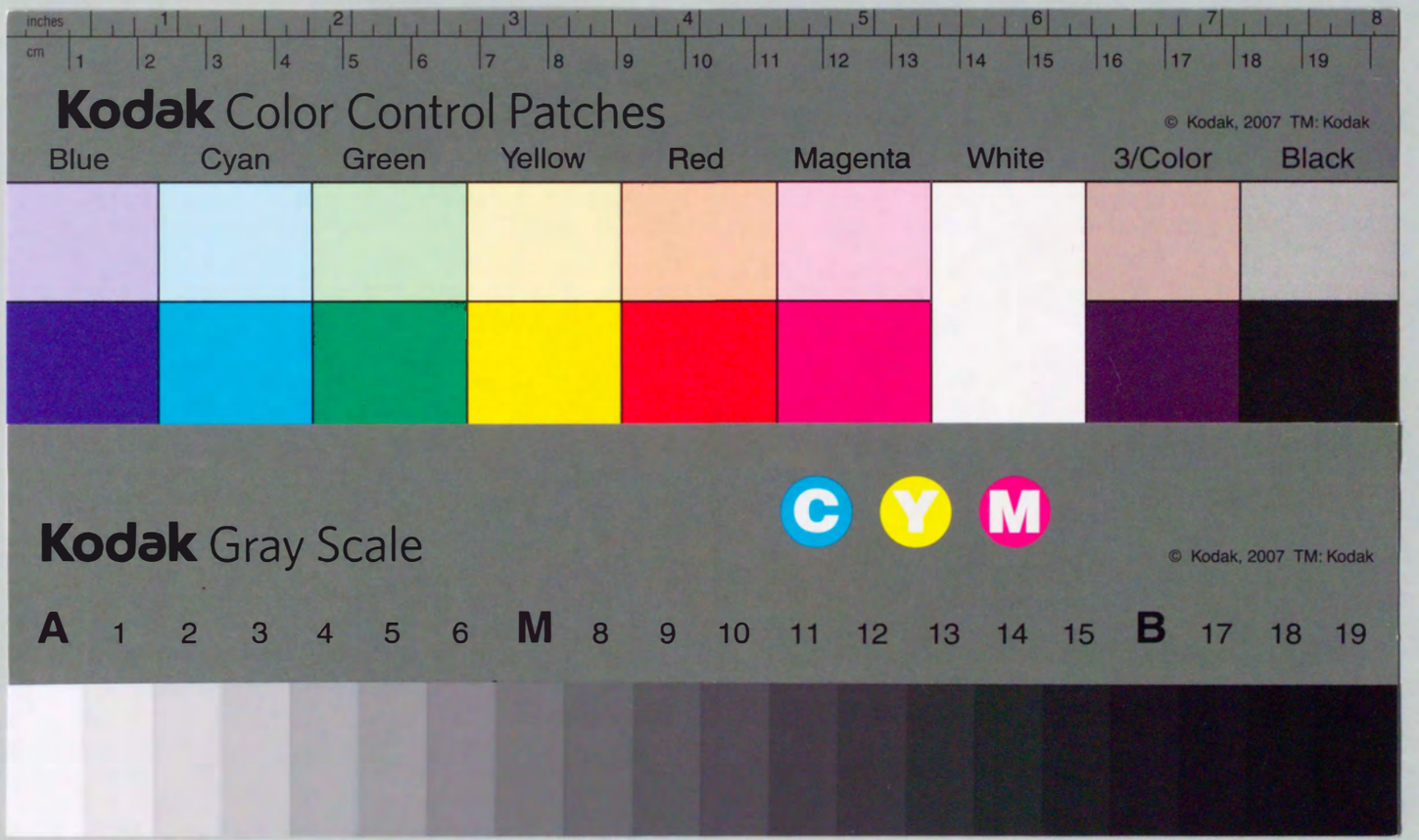
inches
cm
Kodak Color Control Patches
© Kodak, 2007 TM: Kodak
Blue
Cyan
Green
Yellow
Red
Magenta
White
3/Color
Black
Kodak Gray Scale
C
Y
M
© Kodak, 2007 TM: Kodak
A 1 2 3 4 5 6 M 8 9 10 11 12 13 14 15 B 17 18 19